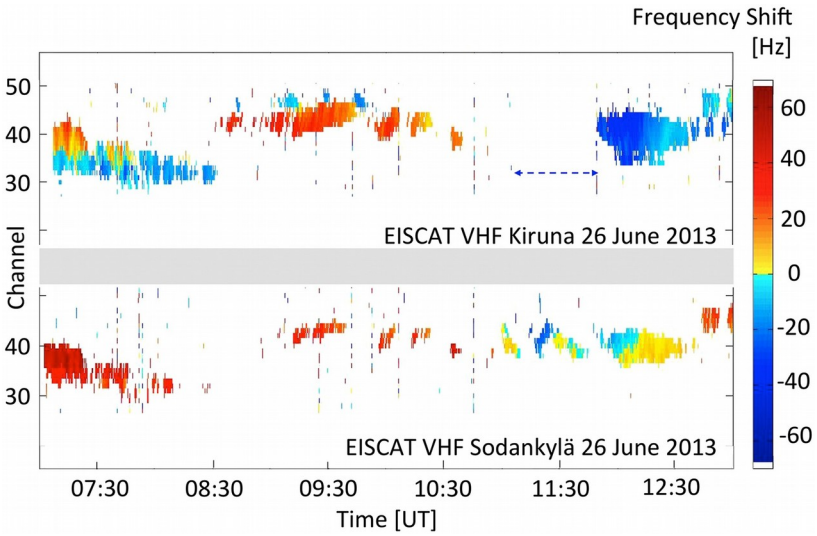

EISCAT

EUROPEAN INCOHERENT SCATTER SCIENTIFIC ASSOCIATION

ANNUAL REPORT 2015 – 2016

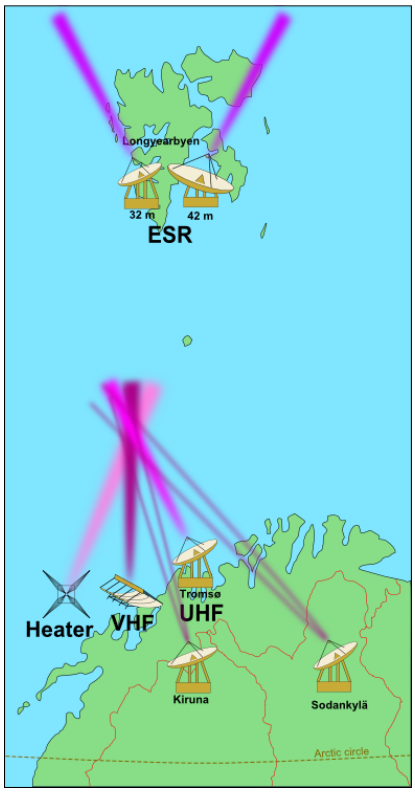

EISCAT Radar Systems

Location		Tromsø	Kiruna	Sodankylä	Longyearbyen	
Geographic coordinates		69°35′N 19°14′E	67°52′N 20°26′E	67°22′N 26°38′E	78°9′N 16°1′E	
Geomagnetic inclination		77°30′N	76°48′N	76°43′N	82°6′N	
Invariant latitude		66°12′N	64°27′N	63°34′N	75°18′N	
Band	UHF	VHF	VHF	VHF	UHF	
Frequency (MHz)	929	224	224	224	500	
Maximum bandwidth (MHz)	8	3	8	8	10	
Transmitter	2 klystrons	1 klystron	-	-	16 klystrons	
Channels	6	6	6	6	12	
Peak Power (MW)	2.0	1.6	-	-	1.0	
Average power (MW)	0.25	0.20	-	-	0.25	
Pulse duration (ms)	0.001–2.0	0.001–2.0	-	-	0.0005–2.0	
Phase coding	binary	binary	binary	binary	binary	
Minimum interpulse (ms)	1.0	1.0	-	-	0.1	
Digital processing	14 bit ADC on IF, 32 bit complex autocorrelation functions, parallel channels					
					Antenna 1	**Antenna 2**
Antenna	parabolic dish	parabolic cylinder	parabolic dish	parabolic dish	parabolic dish	parabolic dish
Feed system	32 m steerable Cassegrain	120 m × 40 m steerable line feed 128 crossed dipoles	32 m steerable crossed dipole	32 m steerable crossed dipole	32 m steerable Cassegrain	42 m fixed Cassegrain
System temperature (K)	90	250	100	100	80	65
Gain (dBi)	48.1	46	48.1	48.1	42.5	44.8
Polarisation	circular	circular	any	any	circular	circular

EISCAT Heating Facility (Tromsø)

Frequency range: 4.0 MHz to 8.0 MHz, Maximum transmitter power: 12×0.1 MW, Antennas: Array 1 (5.5 MHz to 8.0 MHz) 30 dBi, Array 2 (4.0 MHz to 5.5 MHz) 24 dBi, Array 3 (5.5 MHz to 8.0 MHz) 24 dBi.
Additionally, a Dynasonde is operated at the heating facility.

Cover picture: Observations of wind shear in polar mesospheric echoes, from the work by I. Mann et al.

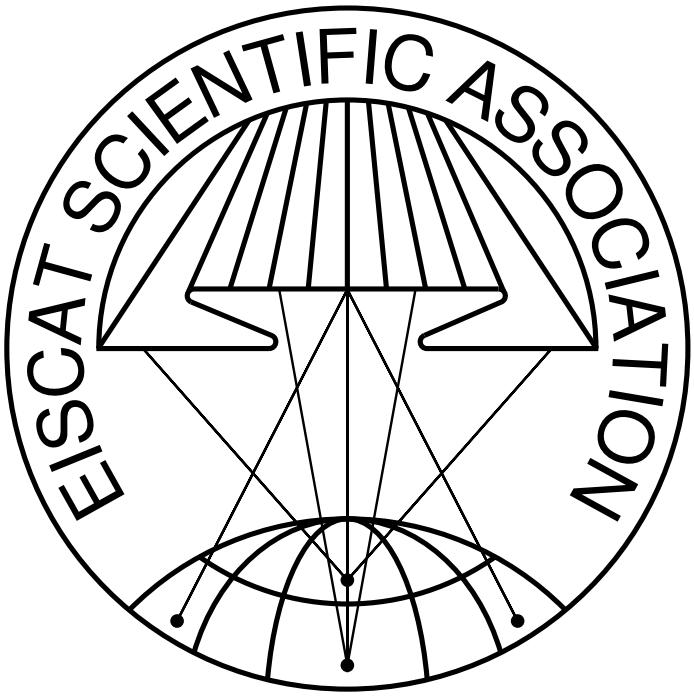

EISCAT Scientific Association
2015–2016

The high-latitude atmosphere and ionosphere represent both a critically important window on solar-terrestrial relationships and a vast natural plasma physics laboratory. The Arctic areas of northern Europe provide the easiest access to this available anywhere in the World, with well-developed infra-structure, extensive installed observational facilities, and a number of centres of academic excellence in appropriate fields.

The EISCAT Scientific Association was established in 1975 and its first incoherent scatter radar system became operational in 1981. Since then, the facilities of the EISCAT Scientific Association have been continuously developed and extended and today comprise world-class radars and a powerful ionospheric heating facility. Developments in hardware, software, and observational techniques have allowed the range of science addressed to be dramatically broadened since the first observations were made and the Association continues to provide and develop appropriate tools to support its user community. Access to the world-class EISCAT facilities is provided to all scientists in the Associate countries and to other Affiliates, and processed data products are made freely available to all. In this way, EISCAT has played a pivotal role in supporting research in many areas including solar-terrestrial relationships, solar system physics, geospace studies, space weather, and global change.

The scientific strategy of EISCAT is to understand the various forms of coupling between the Sun, the interplanetary medium, the terrestrial magnetosphere, ionosphere, and atmosphere of the high-latitude regions, natural and anthropogenic forcing, and related plasma physics and dynamics, and to achieve the necessary knowledge, understanding, principles, and techniques which would allow mankind to monitor, predict, and mitigate such processes within the next 30 years.

The specific goals of EISCAT are to develop large-scale facilities, techniques, and methods and, together with other ground-based and space-borne instruments, and as part of the global network of incoherent scatter and other middle and upper atmosphere radars, to encourage and undertake high quality research related to the global goal through studies addressing:

- *Behaviour and energy budget of the high-latitude regions, including space weather effects*
- *Fundamental plasma physics and dynamic processes in the near-Earth space environment*
- *Trends in atmospheric and ionospheric conditions, including long term/global change*
- *Properties and dynamics of the interplanetary environment*
- *Parametrisation of these processes and the development of techniques for their prediction*

The investments and operational costs of EISCAT are shared between:

China Research Institute of Radiowave Propagation, People's Republic of China
National Institute of Polar Research, Japan
Natural Environment Research Council, United Kingdom
Norges forskningsråd, Norway
Suomen Akatemia, Finland
Vetenskapsrådet, Sweden

Contents

The chairman's section

During 2015 and 2016, EISCAT Council held its regular meetings in Kiruna, Sweden (meeting 84), Hainan, China (meeting 85), Tromsø, Norway (meeting 86) and Oxford, UK (meeting 87). There was also one extraordinary meeting by teleconference, dictated by the need to take urgent decisions about the funding for the EISCAT_3D project. In addition a number of "round tables" and sub-committees, involving several of the Council members, were meeting during this period, to regularly review the funding situation for EISCAT_3D and to review its planned data policy.

These years turned out to be pivotal ones for the EISCAT Scientific Association. At the start of 2015, EISCAT was still involved in quite intense discussions about the national capital funding contributions for EISCAT_3D. At that point, only Sweden had made a firm capital pledge to commit money to construction, though discussions in Norway and Finland were at a very advanced stage, a status which in itself represented the culmination of several years of detailed negotiations. Regular round-table discussions were being held between the various national partners and firm funding commitments from Norway and Finland quickly followed, so that by the first Council meeting of 2015, we already had pledges for around 70 % of the required capital money, with further discussions of national funding contributions ongoing in the UK and Japan. Significant work was also being done in Kiruna to establish the detailed costs of the various parts of the project and Council approved the concept that these should be captured in a "cost book" which would reflect EISCAT's opinion of what each element of the project should cost, so that tenders could be benchmarked against this. Also at the beginning of 2015, we found out that EISCAT had secured EU funding for its "Preparation for Production" (PfP) study, and discussion of the progress of this study became a significant element of the discussions in the Council meetings which followed.

The year 2016 brought further positive news for EISCAT_3D construction, in that the UK became increasingly positive about its ability to make a national contribution of capital funds (finally confirmed early in 2017), with Japan also making a small amount of funding available for the development of solid state transmitters. Initial discussions began with the US National Science Foundation about its possible future interest in EISCAT_3D. Final locations for the first three EISCAT_3D sites were selected and discussions began between the various computing and internet authorities in the Nordic countries about the required computing and network infrastructure. In addition there were several detailed discussions of how satellite and space debris echoes in EISCAT_3D data should be handled, given their potentially sensitive nature. A working group was constituted, which formulated a new policy which was eventually approved as being acceptable to all of the relevant authorities.

By the end of 2016, it looked almost certain that EISCAT would be in a position where around 86 % of the capital investment had been pledged, though this would not be confirmed until the following spring. Although the pledges made for the Norwegian, Swedish and Finnish contributions were due to lapse at the end of 2016, agreement was secured to extend these into 2017, by which time the status of the potential UK and Japanese contributions would be clearer, with the anticipation that the go-ahead could be given at that point. In summary, from the unclear position at the beginning of 2015, the situation had changed to one in which we had relatively high confidence that the go-ahead would be given in 2017 for the EISCAT_3D project to finally move ahead into the construction phase.

There were a few other matters which also occupied Council's thoughts during this period. The issues of interference on the EISCAT UHF and VHF systems continued to be a topic for discussion, though the situation did not become bad enough to make either of the mainland systems unusable. Council also discussed the need to promote the increased use of the EISCAT Svalbard Radar. Because of changes in the land lease arrangements, the decision was taken to mothball the Svalbard

Dynasonde. The revived EISCAT Administration and Finance Committee moved from being a somewhat "ad hoc" body to being once again a full part of the EISCAT committee structure, with Meri Vannas being appointed as its first regular Chair, and Dr. Thomas Ulich becoming the chair of SAC. Although funding for EISCAT operations remained tight, the regular budget of the Association continued to break even, while delivering an acceptable amount of radar data. Council also took the very pleasing decision to award a well-deserved Beynon Medal to Prof. Ryo Fujii. Most importantly, Dr. Craig Heinselman signed a new three-year contract as EISCAT Director for the period 2016-2019.

On a personal note, it was a pleasure to chair EISCAT Council during this important period and thanks are due to several people for their support, in particular to Prof. Hiroshi Miyaoka for his support as vice-chair and to Henrik Andersson for his excellent work in preparing the meeting papers and accounts which were critical to our decision-making in this important period.

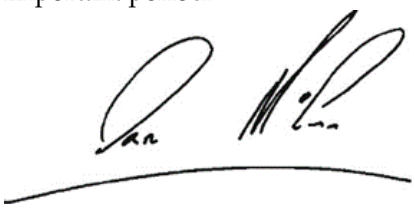

Ian McCrea
STFC Rutherford Laboratory
Council Chair 2015 and 2016

Director's pages

EISCAT continues to provide its user community with incoherent scatter radar (ISR) systems of the highest technical quality at key locations in the Geospace environment. Continuing to push the limits of our capabilities, a group headed by the University of Oulu implemented and tested a quadri-phase coding experiment on the UHF system and produced a pair of reports about those results. While the overall measurement improvements from the chosen codes were modest, the investigators showed that this capability represents an additional coding dimension for ISR measurements in the future. It also points toward needing as much modulation flexibility as possible/affordable in the EISCAT_3D system planning.

On the mainland, both the UHF and VHF radars operate at approximately 1.5 MW of peak power, albeit with no spare klystrons (though there is a fallback option in the case of a UHF klystron failure). Frequency allocation protection is also a growing challenge on the mainland due to cellular telephone operators at UHF and digital audio broadcast (DAB) operators at VHF. The DAB issue, in particular, has forced us to modify our operating modes to use the portion of our spectrum that is free of unwanted signals.

The European Commission granted EISCAT funding for a new project under the Horizon 2020 call: EISCAT_3D Preparation for Production (EISCAT3D_PfP). The overall objective of this project is to facilitate a smooth and swift transition of EISCAT_3D from the FP7 Preparatory Phase project toward its implementation. EISCAT3D_PfP will collaborate with engineering companies, electronic manufacturers and other industrial partners and SMEs to fulfil its overall design goals. An important first step in the technical integration and system testing is setting up a test-bed made up of an array consisting of 91 antenna elements. This Test Subarray will be used to test manufacture-ready sub-assemblies, low-level software, and the integration/interoperability of the system components prior to launching full scale implementation. The total budget is in excess of 3 MEuros and includes project management, coordination, and contracted work. The major budget fraction contains the procurement of production-ready designs and hardware.

The EISCAT3D_PfP project has been running smoothly, though with a delay in the startup due to the need to establish proper contracts through a tendering process. Four additional staff were hired and now work on that project full time. The first external contract was written with a consultant firm to help the project utilize tendering practices that match industry expectations. Part of this effort included constructing a documentation model using a standard system modeling language (SysML). In the end, contracts were signed for hardware for both a First Stage Receive Unit and for an Antenna Unit, in addition to the contract for the consulting firm.

Funding efforts toward the full EISCAT_3D implementation have progressed apace. The project has a combination of positive funding decisions and other indications of future commitments from Finland, Norway, and Sweden. It is also being positively received as part of Japan's Roadmap 2014, though no funds have yet been attached to that roadmap. A group from EISCAT Headquarters and the University of Tromsø also identified a promising location for the transmitter array in Skibotn valley in Norway. This site is flat and sufficiently large to accommodate the core array and, according to the landowner (Norwegian governmental organization Statskog), it is available for use. It has some natural RF protection from interfering Digital Audio Broadcast transmitters due to the local terrain.

EISCAT is also receiving support for EISCAT_3D via a project with the Nordic e-Infrastructure Collaboration (NeIC). This project is advising us about high-bandwidth connectivity to the three initial sites as well as with possible architectures for data processing and data archiving.

After extended consideration, Council decided to terminate the EISCAT Svalbard Radar 3rd Antenna project. The reasons for that termination included the very high projected costs of operation

as well as the need to concentrate staff and effort on the EISCAT_3D project at this time. This action does not in any way reduce EISCAT's commitment to the continued operation of the ESR systems and, in fact, a decision was made to purchase 10 additional klystrons to help ensure its long-term viability. When added to the 3 used tubes with low numbers of operational hours, this should fulfil our needs for approximately a decade of normal operations, at which time a new transmitter design, at least, will likely be needed.

EISCAT added two new Affiliates this year, both from South Korea: Korean Polar Research Institute (KOPRI) and Korean Astronomy and Space Science Institute (KASI). This brings the total number of Affiliates to five, including Arctic and Antarctic Research Institute (AARI, Russia), Institute of Radio Astronomy (IRA, Ukraine), and Institut de Recherche en Astrophysique et Planétologie (IRAP, France). It is gratifying to have such wide-reaching international involvement in the EISCAT scientific user community.

EISCAT was very honored to receive an award from the Royal Astronomical Society in the U.K. The award was given to the EISCAT "[...] Team which, since 1975, has made an unparalleled contribution to understanding the solar wind-magnetosphere-ionosphere coupling and the detailed physics of ionospheric behaviour".

Craig Heinselman
Director
EISCAT Scientific Association

Current events

The EISCAT3D_PfP project

EISCAT_3D will be a multi-static phased array radar system dedicated to observations of the coupling of Earth's atmosphere to space in the European sector of the Arctic regions. The EISCAT3D_PfP project functions as a critical step toward reaching production readiness for a design of the EISCAT_3D system that, in a cost- and energy-efficient way, achieves the goals that were described by the scientific community in the Preparatory Phase project's EISCAT_3D Science Case. EISCAT3D_PfP is a two-year project that started in September 2015, and is supported by the European Commission through the Horizon 2020 funding programme.

The overall objective of the project, with the full name "EISCAT_3D: Preparation for Production", is to facilitate a smooth and swift transition of the EISCAT_3D project from the Preparatory Phase to its implementation. The eventual system will be owned by EISCAT Scientific Association, the Coordinator of the previous EISCAT_3D Preparatory Phase project which was completed in September 2014 and achieved the major requirements for implementing EISCAT_3D.

EISCAT3D_PfP involves collaboration with engineering companies, electronic manufacturers and other industrial partners and SMEs to bridge from the FP7 Preparatory Phase toward the efficient implementation of this new research infrastructure. An important first step in the technical integration and system testing is setting up a testbed made up of an array consisting of 91 antenna elements. This Test Subarray will be used to test manufacture-ready sub-assemblies, low-level software, and the integration/interoperability of the system components prior to launching full scale production of the 9919 antenna elements in the transmitter/receiver array as well as the 19 838 antenna elements for two receiver arrays in the first stage of the EISCAT_3D implementation. This project will speed the transition from engineering prototypes to production readiness so EISCAT_3D can quickly reach a mass producible instrument configuration that is cost-effective, energy efficient and easy to maintain. The Test Subarray will also be used for systems integration tests and for implementation of the subarray beam forming in order to verify the performance of the entire array.

The main tasks to reach the project's objective are:

- Carrying out engineering work in collaboration with industry to finalise the design of critical subsystems of the EISCAT_3D instrument
- Developing and procuring a Test Subarray for EISCAT_3D and assembling it in the Arctic environment.
- Developing dedicated engineering-level software.
- Verifying and validating the performance of the Test Subarray and developing protocols for the construction and commissioning of EISCAT_3D.

The EISCAT3D_PfP project started with a kick-off meeting and a technical workshop held at EISCAT headquarters in Kiruna, an event attended by EISCAT staff as well as representatives from Swedish Institute of Space Physics, Luleå Technical University and two consulting firms. The meeting presentations and discussions were focused on the overall project, its connections to other EISCAT activities, and the present status of the technical design of the EISCAT_3D system.

Consoden AB, a Swedish company, was selected, after a tendering exercise, as the manufacturing consultant contractor. This consultant firm is supporting the procurement activities in this project that will lead to an efficient implementation and testing of the EISCAT_3D Test Subarray at EISCAT's Ramfjordmoen site, near Tromsø in Norway.

The main achievements towards reaching the project's objective are:

- The technical specifications of the critical subsystems of the EISCAT_3D Test Subarray have been finalised.

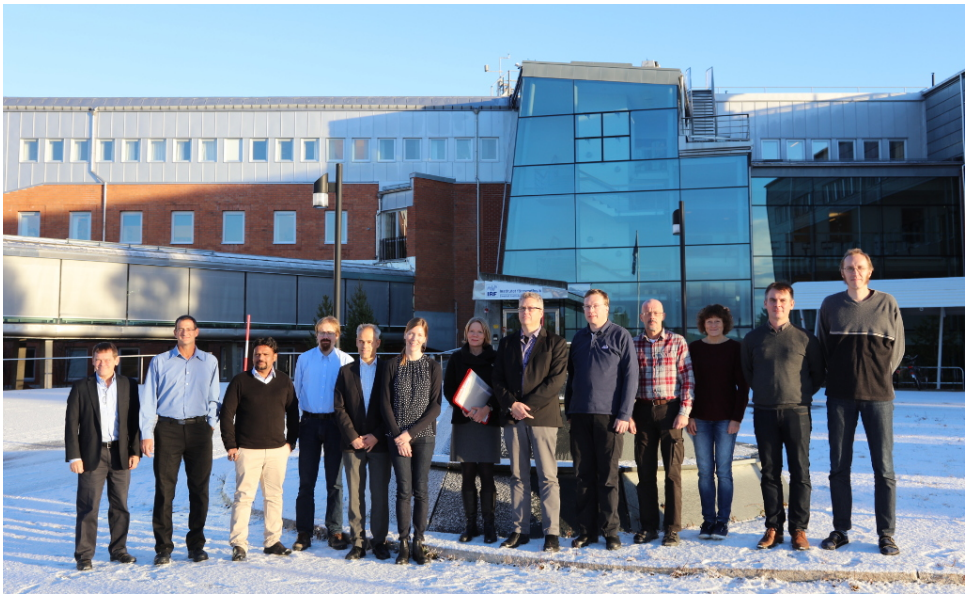

The EISCAT3D_PfP kick-off meeting was held at EISCAT Headquarters in Kiruna, Sweden, on 22–23 October 2015.

- The procurements of the main items for the Test Subarray are underway.
- The sub-systems will have a sub-system manager (SUBMAN) interface and the required engineering-level software needed to communicate with the different SUBMAN's will be developed by the staff in this project. The process of developing this software has started.

Outreach activities during the first year of the project have consisted of participation and presentations in meetings with the scientific community, with policy makers and with industry. The general public has also been reached through coverage in local newspapers and a news item broadcast in Swedish national public radio. Furthermore, quarterly newsletters are published on the project home page as a dissemination tool for the project activities.

The ambition of the EISCAT3D_PfP project is to connect existing knowledge in radar-, electronic- and systems engineering to produce beyond state of the art radar solutions by utilising the competence from several actors in industry, academia and the civil society. The basic technologies behind EISCAT_3D have been used in scientific, civilian and military radar systems since the 1970s. However, EISCAT_3D is the first attempt to combine high-power phased array radar technology with large off-set between the transmitters and receiver arrays and with simultaneous multi-beam capabilities at wide receive bandwidths. To achieve this, EISCAT has developed new ways to integrate radar technologies, electrical and systems engineering advances, high-performance computing and data integration. The combined knowledge to take the system design to blueprints ready for production exists today in industry, academia and civil society in Europe and EISCAT's Asian partner countries, but not necessarily at one single provider. During the preparations for EISCAT_3D, EISCAT Scientific Association established collaborations with SMEs and international engineering companies as well as with civil agencies with a responsibility for innovation procurement. Within the EISCAT3D_PfP project EISCAT takes these collaborations further. By collaborating with national agencies, EISCAT uses innovation procurement to establish cooperation with SMEs and international engineering companies to develop and test components ready for industrial scale production to be used at the EISCAT_3D radar sites.

The collaboration on EISCAT_3D will certainly bring benefits to the future users of the system as they will gain access to a world leading and cost-efficient system for studies of the Arctic/sub-Arctic atmosphere and near-Earth space environment. Simultaneously, it will raise the competence in civil society for the use of innovation procurement and the competitiveness of the industry partners within fields such as radar-, electronic- and systems engineering.

Scientific highlights and list of publications 2015–2016

Ionospheric and atmospheric composition and dynamics

Wind shear observation in PMSE

Mann et al. 2016 presented some of the first data from the newly configured 224 MHz VHF tri-static system. In the mesosphere water ice particles below the optically observable size range participate in the formation of strong radar echoes, which are commonly called Polar Mesospheric Summer Echoes, PMSE. The experiment focused on observations of wind shears during PMSE events. For this study, both the VHF and UHF radar were operated simultaneously and VHF backscattering was received in Kiruna and Sodankylä. The geometry for the experiment is shown in Figure 1, with the two remote receivers intersecting the VHF beam at several different mesospheric altitudes from 68 km to 101 km. By observing the frequency shift of the backscatter power (Hz) compared to the transmission frequency they were able to observe the horizontal motion within the PMSEs. Similar PMSE patterns were found in all three VHF receivers and, in line with previous observations, no evidence of PMSEs were found in the UHF data. Figure 2 shows data from the two remote VHF recievers at Sodankylä and Kiruna over 3 h from 07:00 UT to 13:00 UT on 26 June 2013 (here channel number can be taken as a proxy for altitude). The observations suggest that the PMSE contains sublayers that move in different directions horizontally, and this points to a Kelvin-Helmholtz instability possibly playing a role in PMSE formation. In addition, electron density measurements derived from the observed incoherent scatter at UHF are, at PMSE altitudes, close to the noise level but possibly indicate reduced electron densities directly above the PMSE.

Mann, I., I. Häggström, A. Tjulin, S. Rostami, C. C. Anyairo, and P. Dalin, "First wind shear observation in PMSE with the tristatic EISCAT VHF radar",

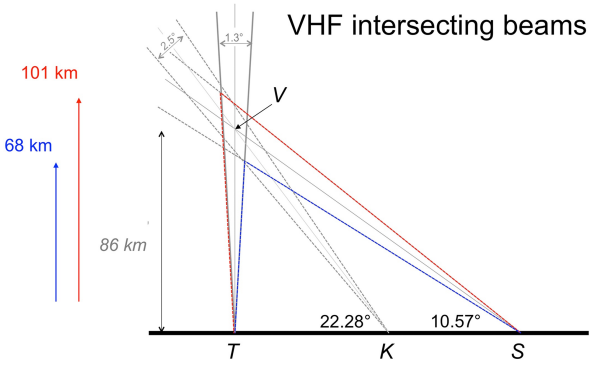

Figure 1: Geometry of receiver antenna cones crossing illuminated volume above Tromsø showing both receiver sight line projected onto the same vertical plane. The antenna sight lines intersect at point V and originate from points T, K, S for Tromsø, Kiruna and Sodankylä respectively. Scattered components are received from any point P within the overlapping volume. For antenna pointing at 86 km the maximum and minimum heights observed from Sodankylä are given.

J. Geophys. Res. Space Physics, 121, 11271–11281, doi:10.1002/2016JA023080, 2016.

Coexisting structures from high- and low-energy precipitation in fine-scale aurora

Dahlgren et al. analysed optical auroral structures and could confirm with help of EISCAT density profiles, that two different high and low energy populations exist:

High-resolution multimonochromatic measurements of auroral emissions (Figure 3) have revealed the first optical evidence of coexisting small-scale auroral features resulting from separate high- and low-energy populations of precipitating electrons on the same field line. The features exhibit completely separate motion and morphology. From emission ratios and ion chem-

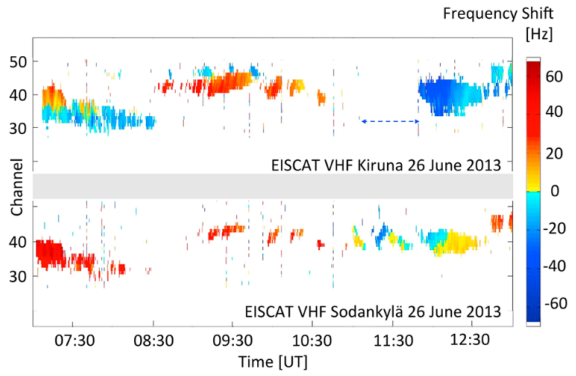

Figure 2: The frequency shift of the backscattered power measured from (top) Kiruna and (bottom) Sodankylä. The channels in the plot were shifted so that the channel number could be used as a proxy for the altitude. A change of the direction of frequency shift with height is best seen in the Kiruna data from 7:10 UT to 7:40 UT and from 9:00 UT to 10:00 UT.

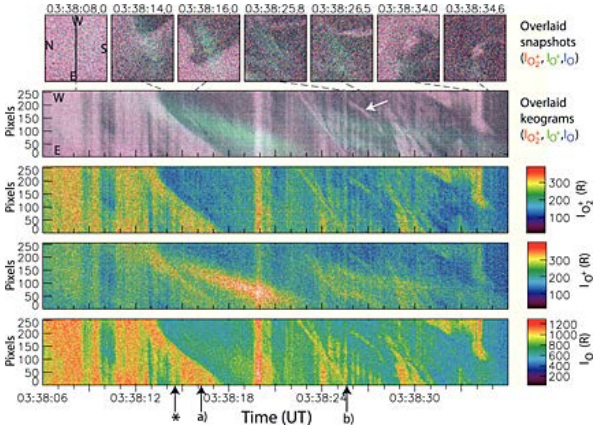

Figure 3: The first row shows snapshots of overlaid ASK images, color-coded $I_{O_2^+}$ (red), I_{O^+} (green), and I_O (blue). The cardinal directions are marked in the first image, together with a line marking the position of the slice used in the time series of slices below. The second to fifth rows show an interval of 30 s, where the second row is the color-coded overlaid slices, followed by $I_{O_2^+}$, I_{O^+}, and I_O in the third to fifth rows respectively.

istry modelling, the average energy and energy flux of the precipitation is estimated. The high-energy precipitation is found to form large pulsating patches of 0.1 Hz with a 3 Hz modulation, and non-pulsating coexisting discrete auroral filaments. The EISCAT density profiles support the finding of energetic electron precipitation of at least 30 keV, with an ionization peak well below 100 km altitude at the time of the pulsating auroral structures, see Figure 4. The low-energy precipitation is observed simultaneously on the same field line as discrete filaments with no pulsation. The simultaneous structures do not interact, and they drift with different speeds in different directions. The study suggests that the high- and low-energy electron populations are accelerated by separate mechanisms, at different distances from Earth. The small-scale structures could be caused by local instabilities above the ionosphere.

H. Dahlgren, B. S. Lanchester, and N. Ivchenko, "Coexisting structures from high- and low-energy precipitation in fine-scale aurora", Geophys. Res. Lett., 42, 1290–1296, doi:10.1002/2015GL063173, 2015.

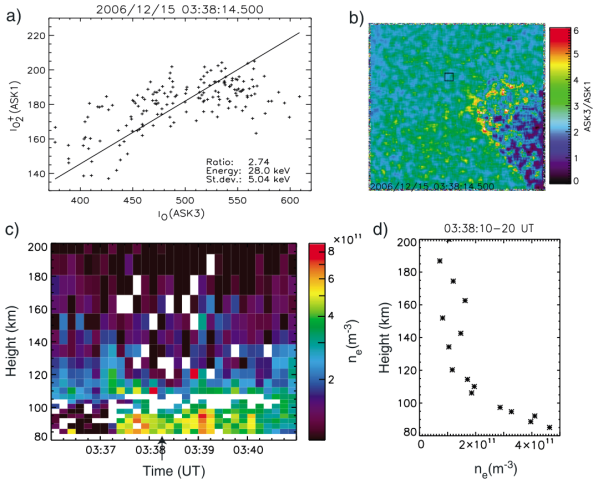

Figure 4: (a) I_O versus $I_{O_2^+}$ per pixel in an area close to magnetic zenith in the ASK images, at 03:38:14.5 UT. (b) This area is marked as a black square in the ratio image shown. A linear fit to the data points give a ratio of 2.7, which corresponds to an energy of the precipitating electrons of about 28 keV. (c) Electron density versus height and time from the EISCAT UHF radar shows an ionization peak below 80 km at the time of the optical observations. (d) The electron density profile at the time marked with an arrow in panel (c), corresponding to the time of the ASK data shown in panels (a) and (b).

High-latitude ion temperature climatology during the International Polar Year 2007–2008

Ion temperature climatology is examined using ionospheric measurements from the European Incoherent Scatter Svalbard Radar (ESR; 78.2°N,

16.0°E) (Figure 5) and the Poker Flat Incoherent Scatter Radar (PFISR; 65.1°N, 212.6°E) during the year-long campaign of the International Polar Year (IPY) from March 2007 to February 2008. The observations were compared against the Thermosphere Ionosphere Electrodynamics General Circulation Model (TIE-GCM), and the International Reference Ionosphere 2012 (IRI-2012) and good agreement was found with the former. Numerical experiments reveal that the daily variation in the high-latitude ion temperature, about 100 K to 200 K, is mainly due to ion frictional heating. The ion temperature increases in response to elevated geomagnetic activity at both ESR and PFISR, in agreement with previous studies. At ESR, a strong response occurs during the daytime, which is interpreted as a result of dayside-cusp heating. It was found that neither model reproduced this response, underscoring the need of improvement in both models at polar latitudes.

Y. Yamazaki, M. J. Kosch, Y. Ogawa, and D. R. Themens,"High-latitude ion temperature climatology during the International Polar Year 2007–2008" J. Space Weather Space Clim., 6, A35, doi:10.1051/swsc/2016029, 2016.

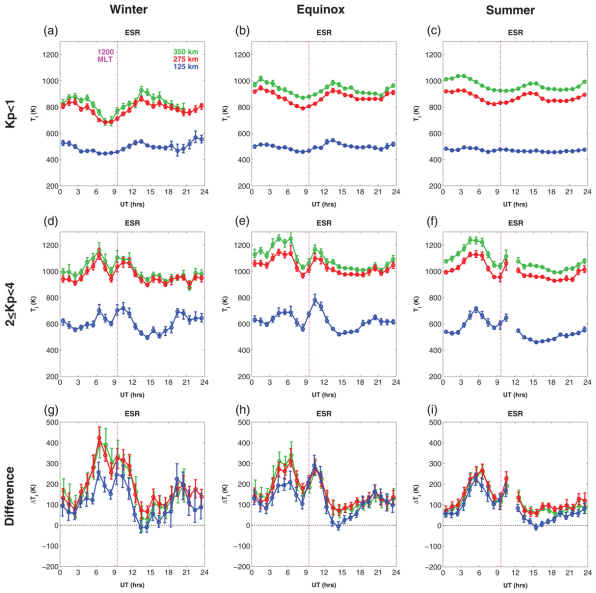

Figure 5: The ion temperature climatology at ESR. Panels (a–c) are for the very quiet condition ($K_{\mathrm{p}} < 1$) and Panels (d–f) are for the moderately active ($2 \leq K_{\mathrm{p}} < 4$) condition. Panels (g–i) show the difference between the results for the moderately active condition and very quiet condition. Panels (a), (d), and (g) are for the winter; Panels (b), (e), and (h) are for the equinox; and Panels (c), (f), and (i) are for the summer. In each panel the green line indicates the result at 350 km; the red line indicates the results at 275 km; and the blue line indicates the results at 125 km. Shading indicates the 95 % confidence interval. The magnetic local time noon is indicated by the vertical magenta line.

Approximate forms of daytime ionospheric conductance

The solar zenith angle (SZA) dependence of the conductance is studied and a simple theoretical form for the Hall-to-Pedersen conductance ratio is developed, using the peak plasma production height. The European Incoherent Scatter (EISCAT) radar observations at Tromsø (67 MLAT) on 30 March 2012 were used to calculate the conductance (Figure 6). The daytime electric conductance is associated with plasma created by solar extreme ultraviolet radiation incident on the neutral atmosphere of the Earth. However, it has been uncertain whether previous conductance models are consistent with the ideal Chapman theory for such plasma productions. We found that the SZA dependence of the conductance is consistent with the Chapman theory after simple modifications. The Pedersen conductance can be understood by approximating the plasma density height profile as being flat in the topside E region and by taking into account the upward gradient of atmospheric temperature. An additional consideration is necessary for the Hall conductance, which decreases with increasing SZA more rapidly than the Pedersen conductance. This rapid decrease is presumably caused by a thinning of the Hall conductivity layer from noon toward night-time. We expressed this thinning in terms of the peak production height in the Chapman theory.

A. Ieda, S. Oyama, H. Vanhamäki, R. Fujii, A. Nakamizo, O. Amm, T. Hori, M. Takeda, G. Ueno, A. Yoshikawa, R. J. Redmon, W. F. Denig, Y. Kamide, and N. Nishitani, "Approximate forms of daytime ionospheric conductance", J. Geophys. Res. Space Physics, 119, 10,397–10,415, doi:10.1002/2014JA020665, 2014.

Mesospheric ozone destruction by high-energy electron precipitation associated with pulsating aurora

Energetic particle precipitation into the upper atmosphere creates excess amounts of odd nitrogen and odd hydrogen. These destroy mesospheric and upper stratospheric ozone in catalytic reaction chains, either in situ at the altitude of the energy deposition or indirectly due to transport to other

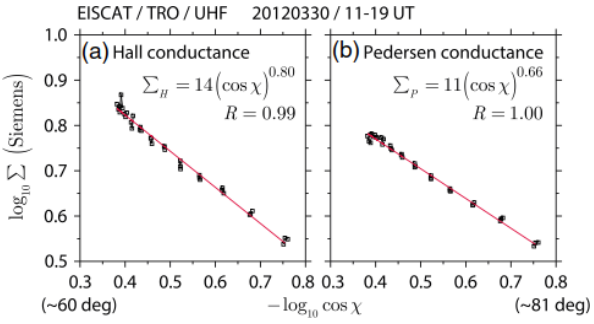

Figure 6: Solar zenith angle, χ, dependence of the conductance, Σ: (a) Hall and (b) Pedersen conductances. Shown is $\log_{10}\Sigma$ against $-\log_{10}\cos\chi$ for one of the data sets. Red lines show the least squares fits to these variables. R is the correlation coefficient.

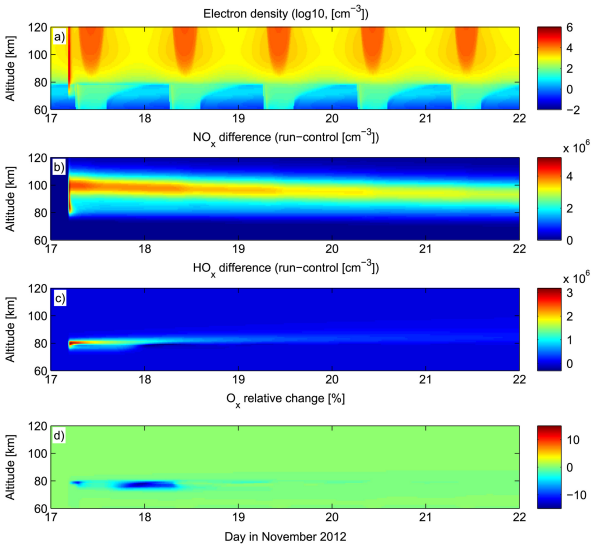

Figure 7: Modelled chemical impact of pulsating aurorae based on a precipitating electron flux spectrum inverted from EISCAT measurement. (a) Modelled electron concentration for the CARD30 scenario. (b) Absolute NO_x difference between CARD30 and control runs, i.e., excess NO_x concentration. (c) Absolute HO_x difference, i.e., excess HO_x concentration. (d) Relative O_x difference.

altitudes and latitudes. Recent statistical analysis of satellite data on mesospheric ozone reveals that the variations during energetic electron precipitation from Earth's radiation belts can be tens of percent. Turunen et al. report model calculations of ozone destruction due to a single event of pulsating aurora early in the morning on 17 November 2012. The presence of high-energy component in the precipitating electron flux (higher than 200 keV) was detected as ionization down to 68 km altitude, by the EISCAT VHF radar. Observations by the Van Allen Probes satellite B showed the occurrence of rising tone lower band chorus waves, which cause the precipitation. The effect of high-energy electron precipitation on ozone concentration was modelled using a detailed coupled ion and neutral chemistry model (Figure 7). Due to a 30 min recorded electron precipitation event 14 % odd oxygen depletion was found at 75 km altitude. The uncertainty of the higher-energy electron fluxes leads to different possible energy deposition estimates during the pulsating aurora event. A depletion of odd oxygen by several tens of percent was found, depending on the precipitation characteristics used in modelling. The effect is notably maximized at the sunset time following the occurrence of the precipitation.

Esa Turunen, Antti Kero, Pekka T. Verronen, Yoshizumi Miyoshi, Shin-ichiro Oyama, and Shinji Saito. "Mesospheric ozone destruction by high-energy electron precipitation associated with pulsating aurora", Journal of Geophysical Research: Atmospheres ,121, 11852–11861, doi:10.1002/2016JD025015, 2016.

Lower thermospheric wind variations in auroral patches during the substorm recovery phase

Measurements of the lower thermospheric wind with a Fabry-Perot interferometer (FPI) at Tromsø, Norway, found the largest wind variations in a night during the appearance of auroral patches at the substorm recovery phase. Taking into account magnetospheric substorm evolution of plasma energy accumulation and release, the largest wind amplitude at the recovery phase is a fascinating result. The results are the first detailed investigation of the magnetosphere-ionosphere-thermosphere coupled system at the substorm recovery phase using comprehensive data sets of solar wind, geomagnetic field, auroral pattern, and FPI-derived wind (Figure 8). This study used three events in November 2010 and January 2012, particularly focusing on the wind signatures associated with the auroral morphology, and found three specific features: (1) wind fluctuations that were isolated at the edge and/or in the darker area of an auroral patch with the largest vertical amplitude up to about 20 m/s and with the longest oscillation period about 10 min, (2) when the convection electric field was smaller than 15 mV/m, and (3) wind fluctuations that were accompanied

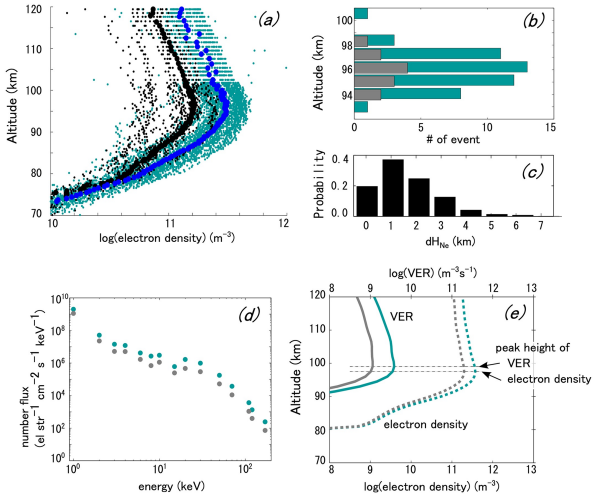

Figure 8: (a) Height profile of the EISCAT-measured electron density (dot: individual 5 s resolved data; solid circle: average), (b) histogram of the peak electron density height shown in panel a, (c) probability of the vertical shift of the peak electron density height, (d) energy flux calculated with the CARD method using mean height profiles shown in panel a, and (e) simulation results of the volume emission rate (557.7 nm) and the electron density (solid and dashed curves, respectively) assuming the CARD energy flux. Horizontal dashed lines are marked at peaks of the two parameters.

by pulsating aurora. This approach suggests that the energy dissipation to produce the wind fluctuations is localized in the auroral pattern. Effects of the altitudinal variation in the volume emission rate were investigated to evaluate the instrumental artifact due to vertical wind shear. The small electric field values suggest weak contributions of the Joule heating and Lorentz force processes in wind fluctuations. Other unknown mechanisms may play a principal role at the recovery phase.

S. Oyama, K. Shiokawa, Y. Miyoshi, K. Hosokawa, B. J. Watkins, J. Kurihara, T. T. Tsuda, and C. T. Fallen, "Lower thermospheric wind variations in auroral patches during the substorm recovery phase", J. Geophys. Res. Space Physics, 121, doi:10.1002/2015JA022129, 2016.

Radar observations of simultaneous travelling ionospheric disturbances and atmospheric gravity waves

Simultaneous observations of atmospheric gravity waves (AGWs) and travelling ionospheric disturbances (TIDs) measured by an incoherent scatter radar at high latitudes are shown. The measurements were made using a beam swing experiment of the EISCAT UHF radar. The F region TID is seen as wavefronts in electron density (Figure 9), whereas the E region AGW is seen in the oscillations of the neutral wind. The wave vector of the TID has a downward component indicating that energy propagates upward. The periods of AGWs and TIDs are approximately the same (52 min to 57 min), so it is concluded that the observed gravity wave in the E region propagates to the F region causing the TID there. Two interesting properties of the waves are observed. First, the neutral wind oscillations have an amplitude minimum at about 115 km. It is suggested that this could be related to the minimum of the vertical refractive index around 120 km. Second, in the course of time, the wave vector of the TID turns more in the downward direction, which leads to an increase in the horizontal wave length from 400 km to 1450 km. A possible explanation is that the background wind increases with altitude and turns the wavefronts more horizontal when distance from a stationary source increases. We suggest that the source is the sunrise terminator, since the horizontal direction of propagation of the TID in the morning hours is from the west, where both the auroral and thunderstorm activity are low.

T. Nygrén, A. T. Aikio, M. Voiculescu, and L. Cai, "Radar observations of simultaneous F region traveling ionospheric disturbances and E region atmospheric gravity waves", J. Geophys. Res. A: Space Physics, 120, 3949–3960, doi:10.1002/2014JA020794, 2015.

Energetic electron precipitation associated with pulsating aurora: EISCAT and Van Allen Probe observations

Pulsating auroras show quasi-periodic intensity modulations caused by the precipitation of energetic electrons of the order of tens of keV. It is expected theoretically that not only these electrons but also sub-relativistic and relativistic electrons precipitate simultaneously into the ionosphere owing to whistler mode wave-particle interactions. The height-resolved electron density profile was observed with the European Incoherent Scatter (EISCAT) Tromsø VHF radar on 17 November 2012. Electron density enhancements were clearly identified at altitudes higher than 68 km in association with the pulsating aurora, suggesting precipitation of electrons with a broadband energy range from about 10 keV up to at least 200 keV. The riometer and network

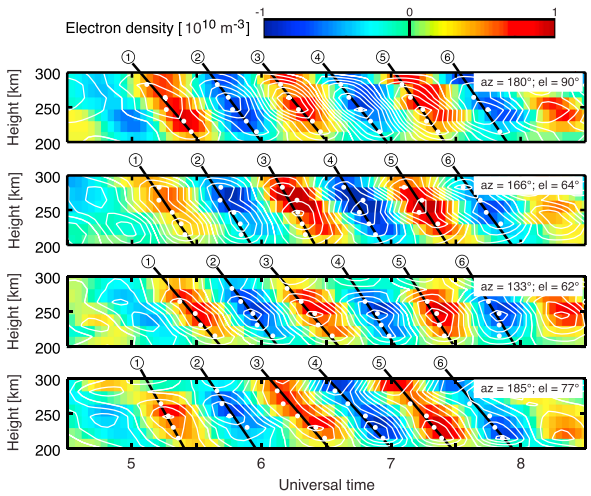

Figure 9: Electron densities for the four beam directions after filtering with a passband 45 min to 75 min. The numbered lines indicate maxima and minima used in the analysis, and the white dots indicate the actual times of each wave crest and trough.

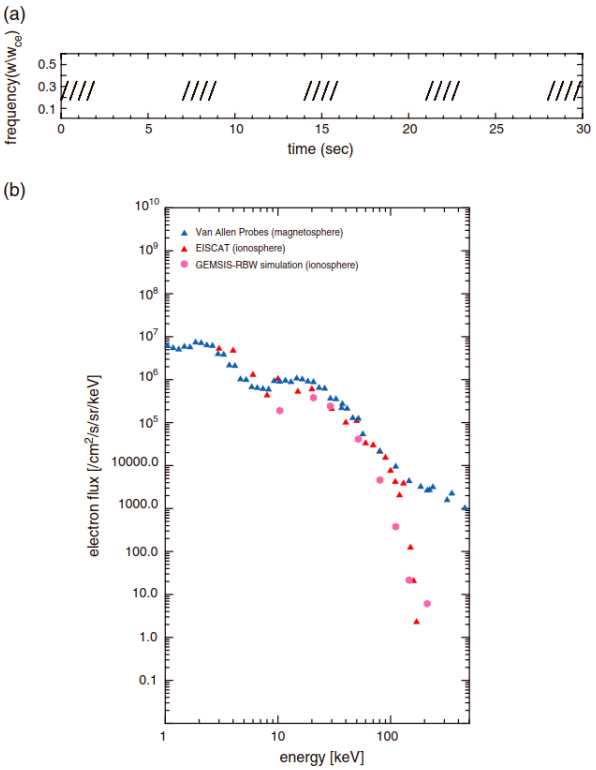

Figure 10: (a) Frequency-time diagram of the LBC waves used in the GEMSIS-RBW simulation. (b) Energy spectrum at the magnetosphere observed by the Van Allen Probe-A satellite (blue triangles), at the ionosphere altitude estimated by the CARD inversion method using the EISCAT observation data (red triangles). Purple hexagons indicate the precipitated flux simulated by GEMSIS-RBW.

of sub-ionospheric radio wave observations also showed the energetic electron precipitations during this period. During this period, the footprint of the Van Allen Probe-A satellite was very close to Tromsø and the satellite observed rising tone emissions of the lower band chorus (LBC) waves near the equatorial plane. Considering the observed LBC waves and electrons, we conducted a computer simulation of the wave-particle interactions. This showed simultaneous precipitation of electrons at both tens of keV and a few hundred keV, which is consistent with the energy spectrum estimated by the inversion method using the EISCAT observations (Figure 10). This result revealed that electrons with a wide energy range simultaneously precipitate into the ionosphere in association with the pulsating aurora, providing the evidence that pulsating auroras are caused by whistler chorus waves. We suggest that scattering by propagating whistler simultaneously causes both the precipitations of sub-relativistic electrons and the pulsating aurora.

Y. Miyoshi, S. Oyama, S. Saito, S. Kurita, H. Fujiwara, R. Kataoka, Y. Ebihara, C. Kletzing, G. Reeves, O. Santolik, M. Cliverd, C. J. Rodger, E. Turunen, and F. Tsuchiya, "Energetic electron precipitation associated with pulsating aurora: EISCAT and Van Allen Probe observations", J. Geophys. Res. Space Physics, doi:10.1002/2014JA020690, 2015.

Auroral ion acoustic wave enhancement observed with a radar interferometer system

Schlatter et al. used the ESR facility complemented by separate receivers for interferometric measurements to study the origin of so-called naturally enhanced ion acoustic lines and associated plasma turbulence:

Measurements of naturally enhanced ion acoustic line (NEIAL) echoes obtained with a five-antenna interferometric imaging radar system are presented. The observations were conducted with the European Incoherent SCATter (EISCAT) radar on Svalbard and the EISCAT Aperture Synthesis Imaging receivers (EASI) installed at the radar site, see Figure 11. Four baselines of the interferometer are used in the analysis. Based on the coherence estimates derived from the measurements, it was shown that the enhanced backscattering region is of limited extent in the plane perpendicular to the

geomagnetic field. Previously it has been argued that the enhanced backscatter region is limited in size; however, here the first unambiguous observations are presented. The size of the enhanced backscatter region is determined to be less than 900 m $\times$ 500 m, and at times less than 160 m in the direction of the longest antenna separation, assuming the scattering region to have a Gaussian scattering cross section in the plane perpendicular to the geomagnetic field. Using aperture synthesis imaging methods volumetric images of the NEIAL echo are obtained showing the enhanced backscattering region to be aligned with the geomagnetic field. Although optical auroral emissions are observed outside the radar look direction, our observations are consistent with the NEIAL echo occurring on field lines with particle precipitation.

N. M. Schlatter, V. Belyey, B. Gustavsson, N. Ivchenko, D. Whiter, H. Dahlgren, S. Tuttle, and T. Grydeland, "Auroral ion acoustic wave enhancement observed with a radar interferometer system", Ann. Geophys., 33, 837–844, doi:10.5194/angeo-33-837-2015, 2015.

Ionospheric variation during pulsating aurora

We have statistically analyzed data from the European Incoherent Scatter (EISCAT) UHF/VHF radars in Tromsø (69.60°N, 19.20°E), Norway, to reveal how the occurrence of pulsating auroras (PsAs) modifies the electron density profile in the ionosphere. By checking five winter seasons' (2007–2012) observations of all-sky aurora cameras of the National Institute of Polar Research in Tromsø, we have extracted 21 cases of PsA. During these PsA events, either the UHF or VHF radar of EISCAT was operative and the electron density profiles were obtained along the field-aligned or vertical direction near the zenith. From these electron density measurements, we calculated $h_{\mathrm{m}}E$ (E region peak height) and $N_{\mathrm{m}}E$ (E region peak density), which are proxies for the energy and flux of the precipitating PsA electrons, respectively. Then, we examined how these two parameters changed during the evolution of 21 PsA events in a statistical fashion. The results can be summarized as follows:

1. $h_{\mathrm{m}}E$ is lower (the energy of precipitation electrons is higher) during the periods of PsA than it is in the surrounding interval
2. When $N_{\mathrm{m}}E$ is higher (flux of PsA electrons is larger), $h_{\mathrm{m}}E$ tends to be lower (precipitation is harder)

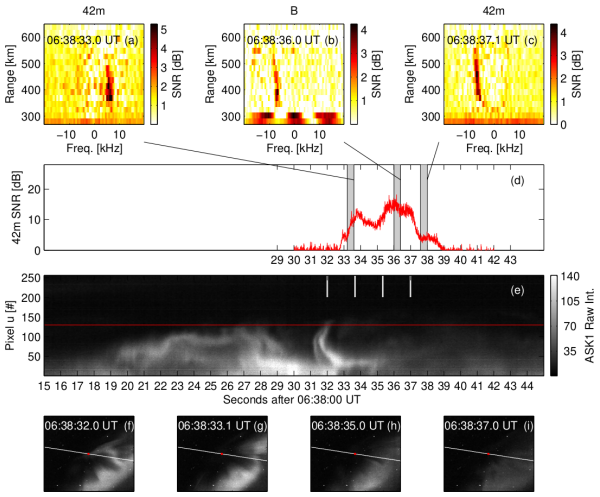

Figure 11: Time history for the NEIAL event observed on 17 December 2012. Panels (a) to (c) show power spectra (400 ms time integration and 22.5 km range gates) obtained with antenna 42 m, B, and 42 m again for the time periods highlighted in panel (d) and centred at 6:38:33.4 UT, 06:38:36.2 UT, and 06:38:37.8 UT. Measurements below 300 km are dominated by ground clutter. Panel (d) shows the signal-to-noise ratio(SNR) of unprocessed and un-decoded data observed with the 42 m antenna. Panel (e) shows a stackplot of intensity as observed with ASK1 along the white line in the snapshots presented in panels (f) to (i), the timing of which is indicated by the white tick marks. The solid red line, panel (e), and red markers, panels (f) to (i), indicate magnetic zenith.

3. $h_{\mathrm{m}}E$ is lower and $N_{\mathrm{m}}E$ is larger in the later magnetic local time
4. When the AE index during the preceding substorm is larger, $h_{\mathrm{m}}E$ is lower and $N_{\mathrm{m}}E$ is larger.

These tendencies are discussed in terms of the characteristics of particles and plasma waves in the source of PsA in the magnetosphere. In addition to the statistics of the EISCAT data, we carried out several detailed case studies, in which the altitude profiles of the electron density were derived by separating the On and Off phases of PsA (Figure 12). This allows us to estimate the true altitude profiles of the PsA ionization, which can be used for estimating the characteristic energy of the PsA electrons and better understanding the wave-particle interaction process in the magnetosphere.

K. Hosokawa, and Y. Ogawa, "Ionospheric variation during pulsating aurora", J. Geophys. Res., doi:10.1002/2015JA021401, 2015.

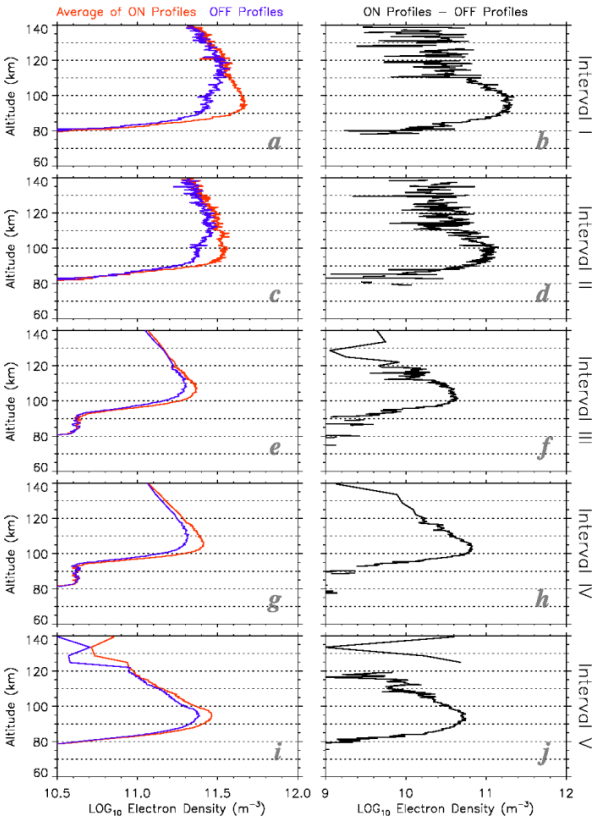

Figure 12: (Left) Altitude profile of the electron density during the On (red) and Off (blue) phases of PsA for intervals I to V, respectively. (Right) Difference between the On and Off profiles in the left panel, which corresponds to the true altitude profile of the electron density at the time of PsA.

Active experiments

Stimulated Brillouin scattering during electron gyro-harmonic heating at EISCAT

This work reports the first EISCAT results of narrowband SEE spectra and compares them to SEE previously observed at HAARP during electron gyro-harmonic heating. An analysis of experimental SEE data shows observations of emission lines within 100 Hz of the pump frequency, interpreted as SBS, during the July 2012 EISCAT campaign. Experimental results indicate that SBS strengthens as the pump frequency approaches the third electron gyro-harmonic. Also, for different heater antenna beam angles, the CUTLASS radar backscatter induced by HF radio pumping is suppressed near electron gyro-harmonics, whereas electron temperature enhancement weakens as measured by EISCAT/UHF radar. The main features of these new narrowband EISCAT observations are generally consistent with previous SBS measurements at HAARP.

H. Y. Fu et al., "Stimulated Brillouin scattering during electron gyro-harmonic heating at EISCAT", Annales Geophysicae 33, 983–990, doi:10.5194/angeo-33-983-2015, 2015.

Horizontal variation of electron temperature under RF heating

Ionospheric modification experiments gives us the opportunity to perform controlled and repeatable experiments investigating the ionospheric response to high power radio waves. Detailed investigations of the horizontal variation of the heated region have hitherto not been done. Earlier studies has investigated the ionospheric response with rather large steps in elevation relative to the Heating beam, and optical methods are somewhat limited in altitude resolution.

During a series of experiments in 2014–2015 we investigated the time and altitude variation of electron temperatures across the Heating beam. By integration of the electron energy equation with a parametrised (time and altitude varying) electron heat source we have made estimates of the characteristic growth times of electron heating (not shown) and the altitude variation at eight elevations around magnetic zenith for the case when EISCAT Heating is transmitting with the beam centred at magnetic zenith. The modelling (second and fourth columns of panels in Figure 13) shows that the ionospheric response (first and third columns) is well described by this model, interestingly with a heat source centred, as expected, at or below the pump wave reflection altitude, except at elevations between 77° and 78.3° where the electron heating centres at altitudes 10 km above the reflection altitude. This can be interpreted as L-mode propagation in the radio window.

Results of ionospheric heating experiments involving an enhancement in electron density in the high latitude ionosphere

The observations of an ionospheric heating experiment with the pump frequencies near the fifth electron gyrofrequency on 11 March 2014 at EISCAT Tromsø site, show the apparent enhancement

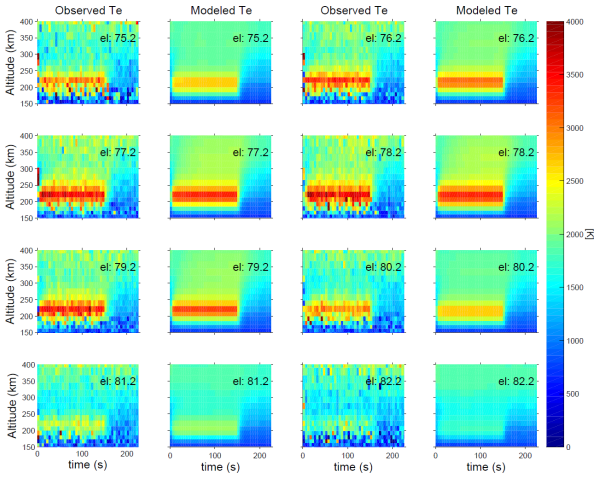

Figure 13: Comparison of observed and modelled ionospheric response to RF heating.

in electron density extending over a wide altitude range and the enhancement in electron temperature around the reflection altitude occurring as a function of pump frequency. In conclusion, the upper hybrid wave resonance excited by the pump wave plays a dominating role and leads to the enhancement in electron temperature at the upper hybrid altitude. The phenomenon of apparent enhancement in electron density does not correspond to the true enhancement in electron density, it may be due to some mechanism remaining to be determined.

WU Jun, WU Jian and XU Zhengwen, "Results of ionospheric heating experiments involving an enhancement in electron density in the high latitude ionosphere"Plasma Science and Technology, Vol.18, No.9, doi:10.1088/1009-0630/18/9/03, 2016.

Preliminary study on active modulation of polar mesospheric summer echoes using radio propagation in a layered dusty plasma in space

The theory of wave propagation in a layered media was used to study the propagation characteristics of an electromagnetic wave at different electron temperatures and to offer a new explanation the active experiment results of Polar Mesospheric Summer Echoes. The simulation results show that the variation tendency of the reflected power fraction is in nice agreement with the results observed by radar at EISCAT. The radar echoes intensity of PMSE greatly decreases with the increase of the radio frequency and the enhancement of the electron temperature.

Zhou Shengguo, Li Hailong, Fu Luyao and Wang Maoyan, "Preliminary study on active modulation of polar mesosphere summer echoes with the radio propagation in layered space dusty plasma", Plasma Science and Technology, Vol.18, No.6, doi:10.1088/1009-0630/18/6/05, 2016.

Parametric instability induced by X-mode wave heating at EISCAT

The EISCAT UHF observations of parametric instability induced by X-mode pump wave at Tromsø, Norway, are presented. Three typical X-mode ionospheric heating experiments on 22 October 2013, 19 October 2012, and 21 February 2013 are investigated in details. Both parametric decay instability (PDI) and oscillating two-stream instability are observed during the X-mode heating period. We suggest that the full dispersion relationship of the Langmuir wave can be employed to analyse the X-mode parametric instability excitation. A modified kinetic electron distribution is proposed and analysed, which is able to satisfy the matching condition of parametric instability excitation. Parallel electric field component of X-mode heating wave can also exceed the parametric instability excitation threshold under certain conditions

X Wang, C Zhou, Moran Liu, F Honary, Binbin Ni, Zhengyu Zhao, "Parametric instability induced by X-mode wave heating at EISCAT", Journal of Geophysical Research: Space Physics, Volume 121, Issue 10, Pages 10536–10548, doi:10.1002/2016JA023070, 2016.

A comparison of overshoot modelling with observations of polar mesospheric summer echoes at radar frequencies of 56 MHz and 224 MHz

In overshoot experiments, where the strength of radar backscatter from PMC can be manipulated by the use of for instance the EISCAT Heating Facility, cases with a substantial reduction in backscatter as the heating is switched on are most common. Theoretical modelling have shown that this is expected for radars with relatively short wavelengths like the EISCAT VHF and UHF radars. The reason being that for the plasma structure sizes reflecting the waves from these two radars, the plasma adjustment time is normally much shorter than the dust charging time as the heater is switched on. For longer wavelengths,

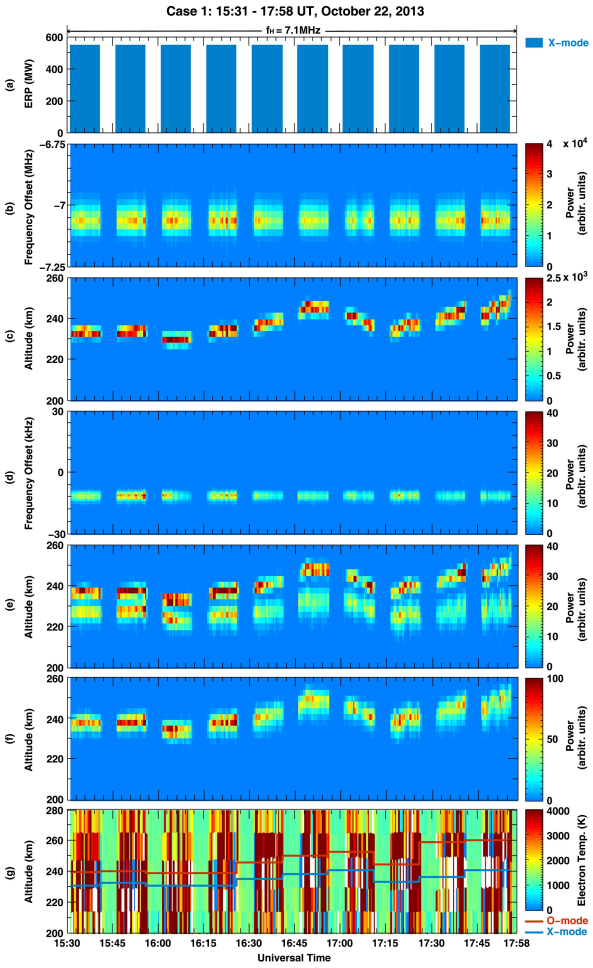

Figure 14: Ionospheric heating experiment at Tromsø from 15:31 UT to 17:58 UT on 22 October 2013 (a) Heater wave consequence and temporal variation of ERP, (b) temporal variations of the undecoded downshifted plasma line in the range of altitudes of 128 km to 302 km with 30 s integration time, (c) temporal-altitude behavior of the undecoded downshifted plasma line with 3 km range resolution and 30 s integration time, (d) temporal variation of HF-induced ion line near reflection height of the pump wave with 30 s integration time, (e) temporal-altitude behavior of the downshifted ion line spectra at −11.9 kHz, (f) temporal-altitude behavior of the upshifted ion line spectra at +11.9 kHz, (g) temporal-altitude behavior of the electron temperature and the solid lines mark the reflection height of the O-mode (red) and the X-mode (blue) heating wave. The plasma line intensity, ion line intensity, and the electron temperature are obtained from the EISCAT UHF radar observation during the heating experiment with 10 min on and 5 min off cycle.

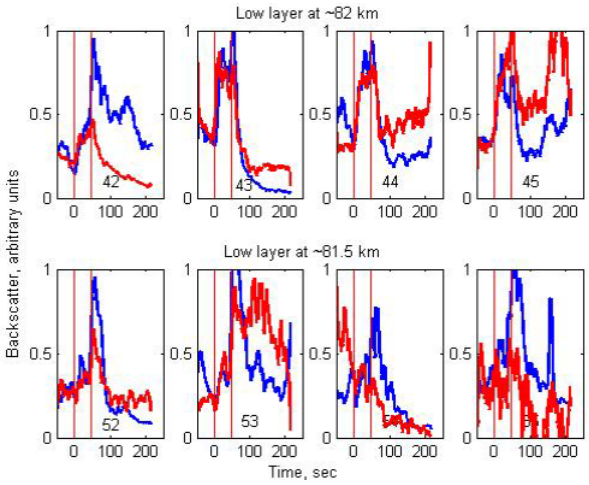

Figure 15: The heater is on at the times between the two vertical red lines. Red lines are for MORRO Radar; blue lines are for the EISCAT VHF Radar.

like for the MORRO radar at 56 MHz, the opposite may be true so that the most rapid process can occasionally be the dust charging. Such a situation can lead to an onset overshoot in which the radar backscatter increases as the heater is switched on. We show statistically that this is confirmed by observations: VHF radar observation show in practically all cases a decrease in backscatter as the heater is switched on, while the MORRO radar shows that a substantial fraction of the cases can have an onset overshoot. We did observe a few very unusual cases where both radars observe nearly identical onset overshoots as the heater is switched on (See Figure 15). This is in contrast to model calculations, which for acceptable dust and plasma conditions predict a substantial difference between observations by the two radars.

O. Havnes, H. Pinedo, C. La Hoz, A. Senior, T. W. Hartquist, M. T. Rietveld, and M. J. Kosch, "A comparison of overshoot modelling with observations of polar mesospheric summer echoes at radar frequencies of 56 MHz and 224 MHz", Ann. Geophys., 33, 737–747, 2015.

Methodology and model validation

Ionosonde measurements in Bayesian statistical ionospheric tomography with incoherent scatter radar validation

We validate 2-D ionospheric tomography reconstructions against EISCAT incoherent scatter radar data. Our tomography method is based on

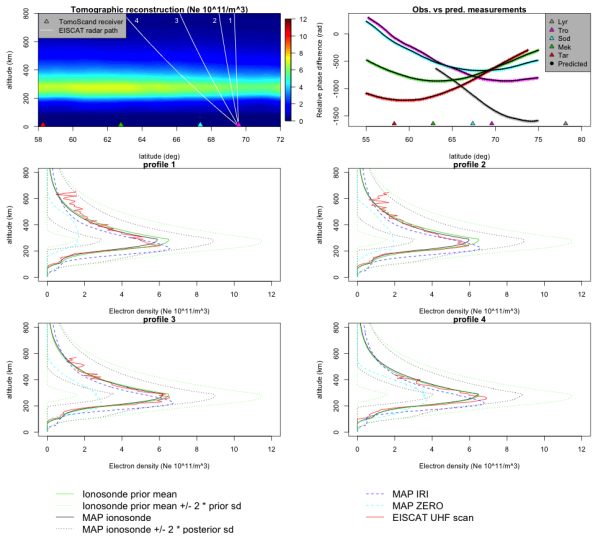

Figure 16: Reconstruction, phase curves and profile comparisons for Overflight III starting at 14 November 2015 13:20 UTC.

Bayesian statistical inversion with prior distribution given by its mean and covariance. We employ ionosonde measurements for the choice of the prior mean and covariance parameters, and use Gaussian Markov random fields as a sparse matrix approximation for numerical computations. This results in a computationally efficient and statistically clear inversion algorithm for tomography.

We demonstrate this method with simultaneous beacon satellite and ionosonde measurements. The performance is compared with results obtained with a zero-mean prior and with the prior mean taken from the IRI2007 model (Figure 16). In validating the results, we use EISCAT UHF radar data as the reference for the ionisation profile shape.

We find that ionosonde measurements improve the reconstruction by adding accurate information about the absolute value and the height distribution of electron density, and outperforms the alternative prior information sources. With an ionosonde at continuous disposal, the presented method enhances stand-alone near real-time ionospheric tomography for the given conditions significantly.

J. Norberg, I. I. Virtanen, L. Roininen, J. Vierinen, M. Orispää, K. Kauristie, and M. S. Lehtinen, "Ionosonde measurements in Bayesian statistical ionospheric tomography with incoherent scatter radar validation", Atmospheric measurement techniques discussions 8 (9), 9823–9851, doi:10.5194/amtd-8-9823-2015, 2015.

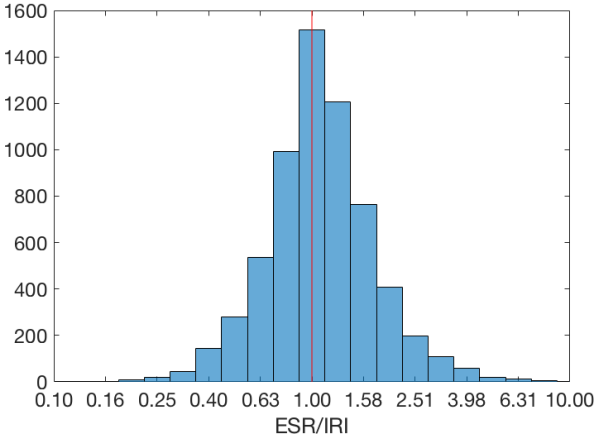

Figure 17: Ratios between ESR electron density estimations and those of obtained from the IRI model.

An evaluation of IRI electron density in the polar cap and cusp using EISCAT Svalbard radar measurements

In this study we used 16 years of measurements from the EISCAT Svalbard radar (ESR) to evaluate F-region electron density estimations from the latest version (2016) of the International Reference Ionosphere (IRI) model. The ESR data were averaged over 3-hour daily intervals for 3-month seasonal periods and in 20 km altitude bins. In each bin the ratio ESR/IRI was calculated. Figure 17 is a histogram showing the distribution of the ratios in all the bins. The results show that the IRI model both overestimates and underestimates the electron density as measured by ESR. Further analysis revealed that the IRI model reproduce the ESR electron density best around the F-peak region. At higher and lower altitudes the model underestimates the electron density, particularly during solar maximum and solar minimum periods. In the period of declining solar activity, 2003–2004, the comparison on the other hand show that for these years the IRI model overestimates the electron density around the F-peak. Also hmF2 and TEC, calculated from the ESR profiles, were compared with the IRI-2016 model. A large discrepancy between ESR-TEC and IRI-TEC was found during the solar maximum 1999–2002, while the hmF2 is slightly overestimated both during solar maximum and solar minimum.

This research is part of the PhD project of Candidate Lindis Merete Bjoland, UiT The Arctic University of Norway Dept. of Physics and Technology.

Inversion of ambient electron density for the modified ionosphere from HF pumping induced plasma cascade lines

In reference to the results obtained during the experiment carried out on 13 September, 2010 at Tromsø, Norway, an inversion method of electron density for the modified ionosphere is developed by using the cascade spectrum obtained by EISCAT VHF radar.

Cheng Musong, Xu Bin, Wu Zhensen, Li Haiying, Wang Zhange, Xu Zhengwen, Wu Jun and Wu Jian, "Inversion of ambient electron density for the modified ionosphere from HF pumping induced plasma cascade lines", Chinese Journal of Radio Science 03(3), 463–469 (in Chinese), 2015.

IONONEST — A Bayesian approach to modeling the lower ionosphere

Martin et al. presented a method of using multifrequency riometer data from the Kilpisjärvi Atmospheric Imaging Receiver Array (KAIRA) instrument to estimate D region height profiles using a nested sampling technique. Their IONONEST technique allowed them to find the posterior probability distribution of parameters that describes an electron density height profile by comparing measured or simulated absorption data to absorption data calculated from a parameterized electron density height profile model. The returned electron density height profiles were compared to data from the EISCAT VHF radar demonstrating that the technique is capable of returning realistic values. They considered two D region models for electron density profiles and found that a polynomial model (model 2 in Figure 18) created more realistic profiles than a two parameter model (model 1).

P. L. Martin, A. M. M. Scaife, D. McKay, and I. McCrea, "IONONEST – A Bayesian approach to modeling the lower ionosphere", Radio Sci., 51, doi:10.1002/2016RS005965, 2016.

Contribution of proton and electron precipitation to the observed electron concentration in October–November 2003 and September 2005

Understanding the altitude distribution of particle precipitation forcing is vital for the assessment of its atmospheric and climate impacts. However, the proportion of electron and proton forcing around

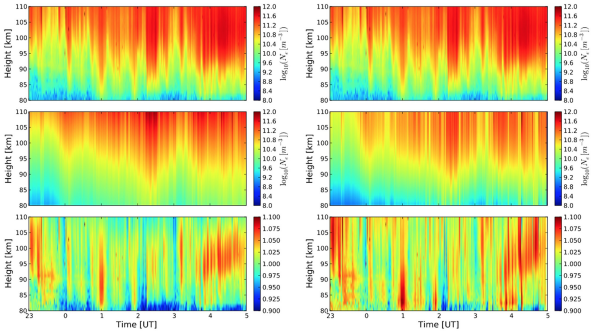

(a) Model 1 (b) Model 2

Figure 18: These plots show a comparison between the height profiles generated using (a) Model 1 and (b) Model 2 fitted to the KAIRA absorption data for the zenith pointing and the height profiles obtained from EISCAT. (top row) The EISCAT height profiles for 23:00 UT on 1 March 2015 until 05:00 UT on 2 March 2015. (middle row) The model height profiles fitted to the KAIRA absorption data for the same time period and pointing. (bottom row) The ratio between the EISCAT data and the fit to KAIRA absorption data. The colour bars are saturated at the extremes in order to emphasize the features

the mesopause region during solar proton events is not always clear due to uncertainties in satellite-based flux observations. Here we use electron concentration observations of the EISCAT incoherent scatter radars located at Tromsø to investigate the contribution of proton and electron precipitation to the changes taking place during two solar proton events. The EISCAT measurements are compared to the results from the Sodankylä Ion and Neutral Chemistry Model (SIC) (Figure 19). The proton ionisation rates are calculated by two different methods — a simple energy deposition calculation and the Atmospheric Ionisation Model Osnabrück (AIMOS v1.2), the latter providing also the electron ionisation rates. Our results show that in general the combination of AIMOS and SIC is able to reproduce the observed electron concentration within $\pm 50\,\%$ when both electron and proton forcing is included. Electron contribution is dominant above 90 km, and can contribute significantly also in the upper mesosphere especially during low or moderate proton forcing. In the case of strong proton forcing, the AIMOS electron ionisation rates seem to suffer from proton contamination of satellite-based flux data. This leads to overestimation of modelled electron concentrations by up to 90 % at altitudes 75 km to 90 km and up to 100 % to 150 % at altitudes 70 km to 75 km. Above 90 km, the model bias varies signi-

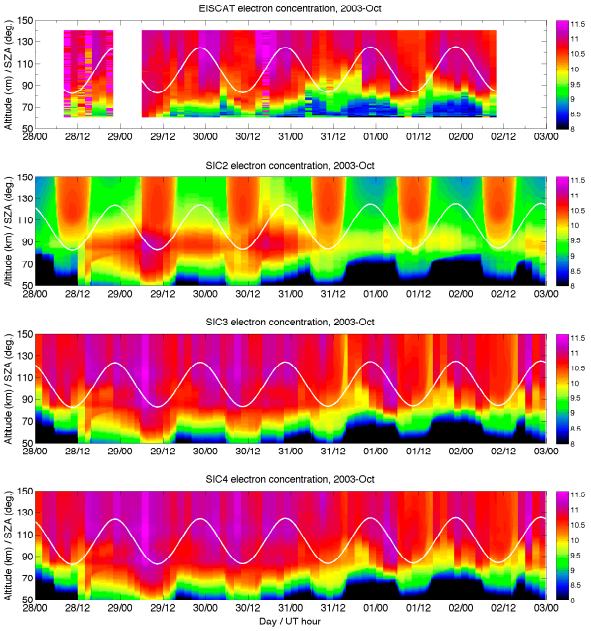

Figure 19: Electron concentrations (10-base logarithm of m^{-3} from EISCAT and three Sodankylä Ion-Neutral Chemistry (SIC) model runs for the October–November 2003 event. The white line shows the diurnal cycle of the solar zenith angle at EISCAT Tromsø.

ficantly between the events. Although we cannot completely rule out EISCAT data issues, the difference is most likely a result of the spatio-temporal fine structure of electron precipitation during individual events that cannot be fully captured by sparse in situ flux (point) measurements, nor by the statistical AIMOS model which is based upon these observations.

P. T. Verronen, M. E. Andersson, A. Kero, C.-F. Enell, J. M. Wissing, E. R. Talaat, K. Kauristie, M. Palmroth, T. E. Sarris, and E. Armandillo, "Contribution of proton and electron precipitation to the observed electron concentration in October–November 2003 and September 2005", Ann. Geophys., 33, 381–394, doi:10.5194/angeo-33-381-2015, 2015.

A theoretical investigation on the parametric instability excited by X-mode polarized electromagnetic wave at Tromsø

Recent ionospheric modification experiments performed at Tromsø, Norway, have indicated that X-mode pump wave is capable of stimulating high-frequency enhanced plasma lines, which manifests the excitation of parametric instability (Figure 20). Theoretical work has been performed to

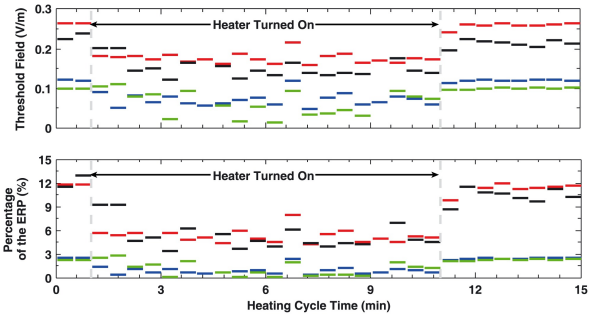

Figure 20: (top) The parametric threshold and (bottom) the percentage between the equivalent ERP of the threshold and the total ERP transmitted from the heater for the experiment on 22 October 2013 (blue), OTSI threshold for the experiment on 22 October 2013 (red), PDI threshold for the experiment on 19 October 2012 (green), and OTSI threshold for the experiment on 19 October 2012 (black); the grey line represents the time when heater is turned off.

investigate how the observation can be explained by the excitation of parametric instability driven by X-mode pump wave.

Xiang Wang, Cannon Patrick, Zhou Chen, Honary Farideh, Ni Binbin and Zhao Zhengyu, "A theoretical investigation on the parametric instability excited by X-mode polarized electromagnetic wave at Tromsø", Journal of Geophysical Research: Space Physics, 121(4), doi:10.1002/2016JA022411, 2016.

Background suppression and strong phase codes in incoherent scatter lag profile inversion

High range resolution incoherent scatter spectra are routinely measured by means of alternating codes and random codes. These radar transmission modulations are cycles of phase-coded pulses whose lagged products form complementary code sets, enabling decoding of incoherent scatter lag profiles by means of matched filtering. Numerically optimised near-perfect modulations are potential successors of the alternating codes and random codes because they enable new measurement techniques, such as so-called multipurpose experiments. The near-perfect modulations cannot be decoded by means of matched filtering, but they are designed for analysis by means of lag profile inversion. Two improvements to this combination are introduced here: Suppression of background noise correlations is implemented as part of lag profile inversion, removing the need for dedicated background measurements, and the concept

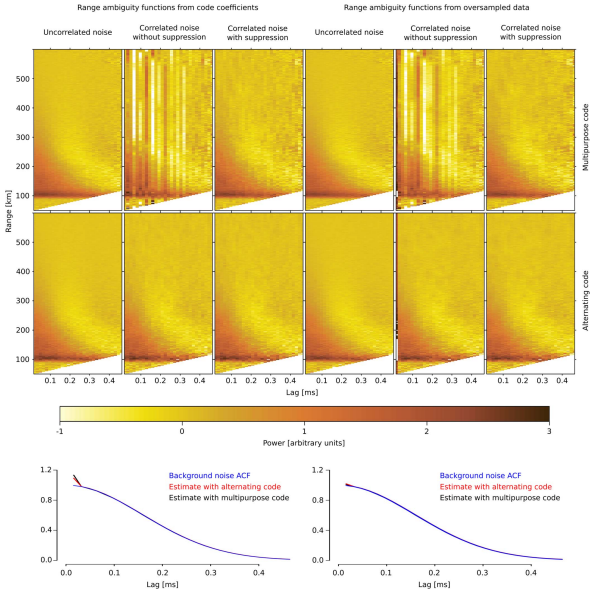

Figure 21: Inverted lag profile matrices from a simulated multipurpose experiment (first row of figure panels) and a simulated alternating code experiment (second row of figure panels). In the first three results at left, range ambiguity functions were calculated from code coefficients, whereas the three results at right were calculated using an oversampled transmitted waveform. Each triplet begins with an inversion result from data that contained only uncorrelated noise, followed by two results with correlated noise contribution — first without and then with the background suppression. The bottom panels contain background autocorrelation function estimates from the lag profile inversion runs. The black curve is from the multipurpose code, the red curve is from the alternating code, and the blue curve is the known true background autocorrelation function. The first lag is elevated from the true curve with both modulations when the code coefficients are used in lag profile inversion.

of strong phase codes is adopted to near-perfect modulations, allowing one to neglect the receiver impulse response in lag profile inversion. See Figure 21.

I. I. Virtanen, "Background Suppression and Strong Phase Codes in Incoherent Scatter Lag Profile Inversion", IEEE Geosci. Remote Sens. Lett., 12, 841–845, doi: 10.1109/LGRS.2014.2363692, 2015.

Historic view, upgrades, and future capabilities

The Science Case for the EISCAT_3D radar

McCrea et al. presented the science case for EISCAT_3D, a next generation phased array using advanced software and data processing techniques. The new radar facility will enable the EISCAT_3D science community to address new, significant science questions as well as to serve society, which is increasingly dependent on space-based technology and issues related to space weather. The location of the radar within the auroral oval and at the edge of the stratospheric polar vortex is also ideal for studies of the long-term variability in the atmosphere and global change.

I. McCrea, A. Aikio, L. Alfonsi, E. Belova, S. Buchert, M. Clilverd, N. Engler, B. Gustavsson, C. Heinselman, J. Kero, M. Kosch, H. Lamy, T. Leyser, Y. Ogawa, K. Oksavik, A. Pellinen-Wannberg, F. Pitout, M. Rapp, I. Stanislawska, and J. Vierinen, "The science case for the EISCAT_3D radar", Progress in Earth and Planetary Science, 2:21, doi:10.1186/s40645-015-0051-8, 2015.

New capabilities of the upgraded EISCAT high-power HF facility

A significant upgrade to the EISCAT Heating facility at the Ramfjordmoen, Tromsø site was undertaken and detailed by Reitveld et al. 2016. It was noted that experimental time on the facility and scientific productivity remains high (it is one of only four similar operational facilities in the world). The new upgrades will increase the scientific capabilities of the system and it is envisaged that experiments will continue until at least the first few years of EISCAT_3D (estimated at the end of 2020). It is also hoped that the new capabilities will provide input for a new HF heating facility for the EISCAT_3D system (located at Skibotn). The improvements are in the areas of radio frequency waveform generation, computer control, and monitoring. In particular, fast stepping in frequency is now possible, an important aspect in examining features close to harmonics of the electron gyrofrequency. One antenna array has been modified to allow reception to implement an HF radar mode for mesospheric and magnetospheric probing. More realistic modelling of the antenna gain gives improved estimates of the total effective radiated power for both wanted

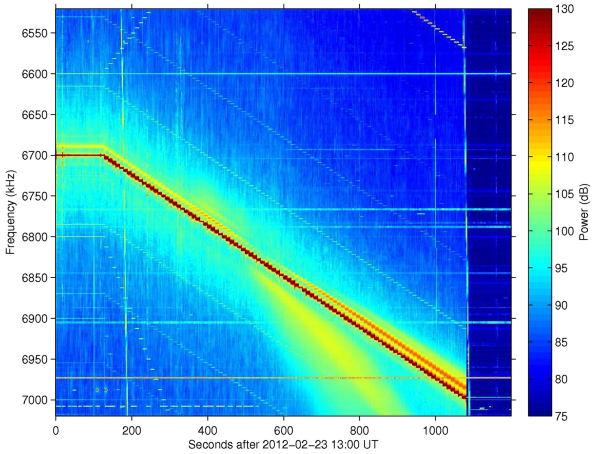

Figure 22: An example of the frequency stepping capability of the new exciter. The spectra of the reflected HF wave and associated stimulated emission sidebands were recorded by a digital sampling receiver 15 km east of the HF facility. The HF carrier was stepped in 3.125 kHz steps every 10 s around the fifth gyroharmonic. Typical SEE features are seen, like the downshifted maximum about 12 kHz below and the broad upshifted maximum increasing in frequency as one steps further above the gyrofrequency, which is at 6.820 MHz at 215 km according to the IGRF model for 2011.

and unwanted circular polarizations. Figure 22 indicates a new frequency stepping capability which will allow scientists to further capitalize on the artificially induced ionospheric effects and fundamental plasma instability research.

Rietveld, M. T., A. Senior, J. Markkanen, and A. Westman, "New capabilities of the upgraded EISCAT high-power HF facility", Radio Sci., 51, doi:10.1002/2016RS006093, 2016.

The forthcoming EISCAT_3D as an extra-terrestrial matter monitor

Pellinen-Wannberg et al. modelled the performance of the planned tristatic EISCAT_3D radar for monitoring dust particle and meteoroids entering the Earth's upper atmosphere:

It is important to monitor the extra-terrestrial dust flux in the Earth's environment and into the atmosphere. Meteoroids threaten the infrastructure in space as hypervelocity hits by micron-sized granules continuously degrade the solar panels and other satellite surfaces. Through their orbital elements meteoroids can be associated to the interplanetary dust cloud, comets, asteroids or the interstellar space. The ablation products of meteoroids participate in many physical and chemical processes at different layers in the atmosphere, many of them occurring in the polar regions.

High-power large-aperture (HPLA) radars, such as the tristatic EISCAT UHF together with the EISCAT VHF, have been versatile instruments for studying many properties of the meteoroid population, even though they were not initially designed for this purpose. The future EISCAT_3D will comprise a phased-array transmitter and several phased-array receivers distributed in northern Scandinavia. These will work at 233 MHz centre frequency with power up to 10 MW and run advanced signal processing systems. The facility will in many aspects be superior to its predecessors as the first radar to combine volumetric-, aperture synthesis- and multistatic imaging as well as adaptive experiments. The technical design goals of the radar respond to the scientific requests from the user community. The VHF frequency and the volumetric imaging capacity will increase the collecting volume compared to the earlier UHF, the high transmitter power will increase the sensitivity of the radar, and the interferometry will improve the spatial resolution of the orbit estimates, see Figure 23. The facility will be able to observe and define orbits to about 10 % of the meteors from the established mass flux distribution that are large or fast enough to produce an ionization mantle around the impacting meteoroid within the collecting volume. The estimated annual mean of about 190 000 orbits per day with EISCAT_3D gives many orders of magnitude higher detected orbit rates than the earlier tristatic UHF radar.

A. Pellinen-Wannberg, J. Kero, I. Häggström, I. Mann, and A. Tjulin, "The forthcoming EISCAT_3D as an extra-terrestrial matter monitor", Planetary and Space Science, 123, 33–40, doi:10.1016/j.pss.2015.10.009, 2015.

Inter-Regional Trade in Research-Based Knowledge: The Case of the EISCAT Radar System

Snickars and Falck investigated interregional and international knowledge trade and how exemplatory a facility like EISCAT is of importance:

This study makes use of a unique micro-database on research performed at the European Incoherent Scatter Scientific Association (EISCAT) radar system to provide some new perspectives on interregional and international knowledge trade

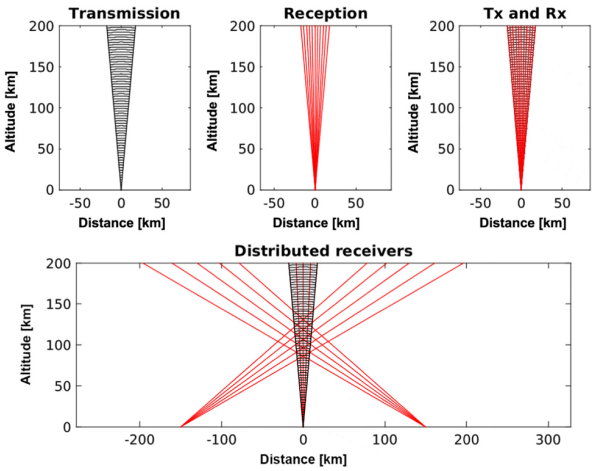

Figure 23: Schematic view of the monostatic transmission and reception (above) and a meteor experiment with, as an example, five transmitted beams and five receiver beamsfrom the close-by receivers.

as regards theory, empirics and practice. More broadly, the study examines the economic and societal importance of EISCAT in a spatial context from the perspective of inter-regional trade of knowledge. The fundamental research question is whether the establishment of such scientific infrastructure leads to clustering of related activities in proximity to its location or whether they are spread world-wide independently of the location. The aim of this study is to illustrate this question with regard to how inter-regional trade in a research-based knowledge system is fashioned. This is also relevant considering the projected investment in a novel EISCAT system, and prior studies emphasizing that highly-skilled professionals are vital in the knowledge-driven economy, influencing the global dynamics of science-based industries and regions.

Folke Snickars and Simon Falck, “Inter-Regional Trade in Research-Based Knowledge: The Case of the EISCAT Radar System” In The Region and Trade pp. 227–264. doi:10.1142/9789814520164_0009, 2015.

Publications 2015

Blagoveshchenskaya, N. F., T. D. Borisova, T. K. Yeoman, I. Häggström, A. S. Kalishin, Modification of the high latitude ionosphere F region by X-mode powerful HF radiowaves: Experimental results from multi-instrument diagnostics, J. Atmos. Sol.-Terr. Phys., 135, 50-63, doi:10.1016/j.jastp.2015.10.009, 2015.

Burrell, A. G., S. E. Milan, G. W. Perry, T. K. Yeoman, and M. Lester, Automatically determining the origin direction and propagation mode of high-frequency radar backscatter, Radio Sci., 50, 1225–1245, doi:10.1002/2015RS005808, 2015.

Cohen, I. J., M. R. Lessard, R. H. Varney, K. Oksavik, M. Zettergren, and K. A. Lynch, Ion Upflow Dependence on Ionospheric Density and Solar Photoionization, J. Geophys. Res. Space Physics, 120, doi:10.1002/2015JA021523, 2015.

Dang, T., J. Lei, X. Dou, and W. Wan, Feasibility study on the derivation of the O+-O collision frequency from ionospheric field-aligned observations, J. Geophys. Res. Space Physics, 120, 6029-6035, doi:10.1002/2015JA020987, 2015.

Dahlgren, H., B. S. Lanchester and N. Ivchenko, Coexisting structures from high- and low-energy precipitation in fine-scale aurora, Geophys. Res. Lett., 42, 1290-1296, doi: 10.1002/2015GL063173, 2015.

Fu, H., W. A. Scales, P. A. Bernhardt, S. J. Briczinski, M. J. Kosch, A. Senior, M. T. Rietveld, T. K. Yeoman, and J. M. Ruohoniemi, Stimulated Brillouin Scattering During Electron Gyro-Harmonic Heating at EISCAT, Annales Geophysicae, 33, 983-990, DOI: 10.5194/angeo-33-983-2015, 2015.

Havnes, O., H. Pinedo, C. La Hoz, A. Senior, T. Hartquist, M. T. Rietveld, M. J. Kosch, A comparison of Overshoot modelling with observations of Polar Mesospheric Summer Echoes at radar frequencies 56 and 224 MHz, Ann. Geophys., Ann. Geophys., 33, 737-747, doi:10.5194/angeo-33-737-2015, 2015.

Havnes, Ove; Pinedo Nava, Henry; La Hoz, Cesar; Senior, Andrew; Hartquist, Tom; Rietveld, Michael T; Kosch, M.J.. Electron Heating Effects on Polar Mesospheric Clouds — A Comparison Between Observations and Modelling. Proceedings of the Cluster and Double Star Symposium — 5th Anniversary of Cluster in Space 2015. ISSN 1609-042X.s 71–77., 2015.

Hosokawa, K., Y. Ogawa, Ionospheric variation during pulsating aurora, , J. Geophys. Res. Space Physics, 120, doi:10.1002/2015JA021401, 2015.

Ishida, T., Y. Ogawa, A. Kadokura, K. Hosokawa, and Y. Otsuka, Direct observations of blob deformation during a substorm, Ann. Geophys., 33, doi:10.5194/angeo-33-525-2015, 525-530, 2015.

Lilensten, J., V. Bommier, M. Barthélemy, H. Lamy, D. Bernard, J. Moen, M. G. Johnsen, U. P. Løvhaug and F. Pitout, The auroral red line polarisation: modelling and measurements, J. Space Weather Space Clim., 5, A26, DOI: http://dx.doi.org/10.1051/swsc/2015027, 2015.

McCrea, I., A. Aikio, L. Alfonsi, E. Belova, S. Buchert, M. Clilverd, N. Engler, B. Gustavsson, C. Heinselman, Johan Kero, M. Kosch, H. Lamy, T. Leyser, Y. Ogawa, K. Oksavik, A. Pellinen-Wannberg, F. Pitout, M. Rapp, I. Stanislawska and J. Vierinen, The science case for the EISCAT_3D radar, Progress in Earth and Planetary Science, 2:21, DOI 10.1186/s40645-015-0051-8, 2015.

D. McKay-Bukowski, J. Vierinen, I. I. Virtanen, R. Fallows, M. Postila, T. Ulich, O. Wucknitz, M. Brentjens, N. Ebbendorf, C.-F. Enell, M. Gerbers, T. Grit, P. Gruppen, A. Kero, T. Iinatti, M. Lehtinen, H. Meulman, M. Norden, M. Orispää, T. Raita, J. P. de Reijer, L. Roininen, A. Schoenmakers, K. Stuurwold, and E. Turunen, KAIRA: The Kilpisjärvi Atmospheric Imaging Receiver Array-System Overview and First Results, IEEE Transactions on Geoscience and Remote Sensing, 53, 3, 1440-1451, 2015.

Miyoshi, Y., S. Oyama, S. Saito, S. Kurita, H. Fujiwara, R. Kataoka, Y. Ebihara, C. Kletzing, G. Reeves, O. Santolik, M. Clilverd, C. J. Rodger, E. Turunen, F. Tsuchiya, Energetic electron precipitation associated with pulsating aurora: EISCAT and Van Allen Probe observations, J. Geophys. Res. Space Physics, 120, DOI: 10.1002/2014JA020690, 2015.

Nygren, T., A. T. Aikio, M. Voiculescu, L. Cai, Radar observations of simultaneous traveling ionospheric disturbances and atmospheric gravity waves, J. Geophys. Res. Space Physics, 120, 3949-3960, doi: 10.1002/2014JA020794., 2015.

Pellinen-Wannberg, A., J. Kero, I. Häggström, I. Mann, A. Tjulin, The forthcoming EISCAT_3D as an extra-terrestrial matter monitor, Planetary and Space Science, 123, 33-44, doi:10.1016/j.pss.2015.10.009, 2015.

Pitout, F., A. Marchaudon, P.-L. Blelly, X. Bai, F. Forme, S. C. Buchert, and D. A. Lorentzen, Swarm and ESR observations of the ionospheric response to a field-aligned current system in the high-latitude midnight sector, Geophys. Res. Lett., 42, doi: 10.1002/2015GL064231., 2015.

Schlatter, N. M., Radar Signatures of Auroral Plasma Instability, Doctoral Thesis, KTH School of Electrical Engineering, Stockholm, Sweden, ISBN 978-91-7595-442-4, 2015.

Schlatter, N. M., V. Belyey, B. Gustavsson, N. Ivchenko, D. Whiter, H. Dahlgren, S. Tuttle, and T. Grydeland, Auroral ion acoustic wave enhancement observed with a radar interferometer system, Ann. Geophys., 33, 837-844, doi:10.5194/angeo-33-837-2015 2015.

Snickars, F. and S. Falck, Inter-Regional Trade in Research-Based Knowledge: The Case of the EISCAT Radar System. In book: The Region and Trade: New Analytical Directions, Chapter: 9, Publisher: World Scientific, Editors: Amitrajeet A Batabyal, Peter Nijkamp, pp.227-264. DOI: 10.1142/9789814520164_0009, 2015.

Spicher, A., W. J. Miloch, L. B. N. Clausen, and J. I. Moen, Plasma turbulence and coherent structures in the polar cap observed by the ICI-2 sounding rocket, J. Geophys. Res. Space Physics, 120, doi:10.1002/2015JA021634, 2015.

Taguchia, S., K. Hosokawaa, Y. Ogawa, Three-dimensional imaging of the plasma parameters of a moving cusp aurora, Journal of Atmospheric and Solar-Terrestrial Physics, 133, 98-110, doi:10.1016/j.jastp.2015.08.012, 2015.

Takahashi, T., S. Nozawa, T. T. Tsuda, Y. Ogawa, N. Saito, T. Hidemori, T. D. Kawahara, C. Hall, H. Fujiwara, N. Matuura, A. Brekke, M. Tsutsumi, S. Wada, T. Kawabata, S. Oyama, and R. Fujii, A case study on generation mechanisms of a sporadic sodium layer above Tromsø (69.6° N) during a night of high auroral activity, Ann. Geophys., 33, 941-953, doi:10.5194/angeo-33-941-2015, 2015.

Tsuda, T. T., S. Nozawa, T. D. Kawahara, T. Kawabata, N. Saito, S. Wada, C. M. Hall, M. Tsutsumi, Y. Ogawa, S. Oyama, T. Takahashi, M. K. Ejiri, T. Nishiyama, T. Nakamura, A. Brekke, A sporadic sodium layer event detected with five-directional lidar and simultaneous wind, electron density, and electric field observation at Tromsø, Norway, Geophys. Res. Lett., 42, doi:10.1002/2015GL066411, 2015.

Verronen, P. T., M. E. Andersson, A. Kero, C.-F. Enell, J. M. Wissing, E. R. Talaat, K. Kauristie, M. Palmroth, T. E. Sarris, and E. Armandillo, Contribution of proton and electron precipitation to the observed electron concentration in October–November 2003 and September 2005, Ann. Geophys., 33, 381-394, doi:10.5194/angeo-33-381-2015, 2015.

Xiong, C., H. Lühr, S. Ma, K. Schlegel, Validation of GRACE electron densities by incoherent scatter radar data and estimation of plasma scale height in the topside ionosphere, Advances in Space Research, 55, 8, 1913-2148, 2015.

Zhang, Q.-H., M. Lockwood, J. C. Foster, S.-R. Zhang, B.-C. Zhang, I. W. McCrea, J. Moen, M. Lester, and J. M. Ruohoniemi, Direct observations of the full Dungey convection cycle in the polar ionosphere for southward interplanetary magnetic field conditions, J. Geophys. Res. Space Physics, 120, doi: 10.1002/2015JA021172., 2015

Publications 2016

Belakhovsky, V., V. Pilipenko, D. Murr, E. Fedorov, and A. Kozlovsky, Modulation of the ionosphere by Pc5 waves observed simultaneously by GPS/TEC and EISCAT, Earth, Planets and Space, 68:102, DOI:10.1186/s40623-016-0480-7, 2016.

Belehaki, A., S. James, M. Hapgood, S. Ventouras, I. Galkin, A. Lembesis, A. Charisi, L. Spogli, J. Berdermann, I. Häggström, The ESPAS e-infrastructure: Access to data from near-Earth space. Advances in Space Research, 58 (7), pp. 1177-1200, DOI:10.1016/j.asr.2016.06.014, ISSN 0273-1177, 2016.

Bjoland, L. M., V. Belyey, U. P. Løvhaug, and C. La Hoz, An evaluation of International Reference Ionosphere electron density in the polar cap and cusp using EISCAT Svalbard radar measurements, Ann. Geophys., 34, 751-758, doi:10.5194/angeo-34-751-2016, 2016.

Borisova, T. D., N. F. Blagoveshchenskaya, A. S. Kalishin, M. T. Rietveld, T. K. Yeoman, and I. Haggstrom, Modification of the High-Latitude Ionospheric F Region By High-Power HF Radio Waves at Frequencies Near the fifth and Sixth Electron Gyroharmonics, Radiophysics and Quantum Electronics, Vol.58, No.8, (Russian Original Vol. 58, No. 8, August, 2015), DOI 10.1007/s11141-016-9629-2, 2016.

Burrell, A. G., T. K. Yeoman, S. E. Milan, and M. Lester, Phase calibration of interferometer arrays at high-frequency radars, Radio Sci., 51, doi:10.1002/2016RS006089, 2016.

Cai, Lei, Electromagnetic energy input to the high-latitude ionosphere, doctoral thesis, University of Oulu, Finland, ISBN 978-952-62-126-6, 2016.

Cai, L., A. Aikio, and S.E. Milan, Joule heating hot spot at high latitudes in the afternoon sector, J. Geophys. Res. Space Physics, 121, doi:10.1002/2016JA022432, 2016.

Chartier, A., B. Forte, K. Deshpande, G. Bust, and C. Mitchell, Three-Dimensional Modeling of High-Latitude Scintillation Observations, Radio Sci., 51, doi:10.1002/2015RS005889, 2016

Haerendel, G., History of EISCAT – Part 4: On the German contribution to the early years of EISCAT, Hist. Geo Space. Sci., 7, 67-72,, 2016.

Havnes, O., and T. W. Hartquist, Nanodust shedding and its potential influence on dust-related phenomena in the mesosphere, J. Geophys. Res. Atmos., 121, 12,363–12,376, doi:10.1002/2016JD025037, 2016.

Hocking, W. K., J. Röttger, R. D. Palmer, T. Sato and P. B. Chilson, Atmospheric Radar, Application and science of MST radars in the Earth's mesosphere, stratosphere, troposphere, and weakly ionized regions, Cambridge University Press, ISBN 978-1-107-14746-1, 2016.

Jin, Y., J. I. Moen, W. J. Miloch, L. B. N. Clausen, and K. Oksavik, Statistical study of the GNSS phase scintillation associated with two types of auroral blobs, J. Geophys. Res. Space Physics, 121, doi:10.1002/2016JA022613, 2016.

Kvammen, A., The volume distribution of artificial aurora induced by HF radio waves in the ionosphere, Masters thesis, UiT The Arctic University of Norway, 2016.

Lu, Z., M. Yao, and X. Deng, An effective method for incoherent scattering radar's detecting ability evaluation, Radio Sci., 51, 852–857, doi:10.1002/2015RS005827, 2016.

Mann, I., I. Häggström, A. Tjulin, S. Rostami, C. C. Anyairo, and P. Dalin, First wind shear observation in PMSE with the tristatic EISCAT VHF radar, J. Geophys. Res. Space Physics, 121, doi:10.1002/2016JA023080, 2016.

Martin, P. L., A. M. M. Scaife, D. McKay, and I. McCrea, IONONEST – A Bayesian approach to modeling the lower ionosphere, Radio Sci., 51, doi:10.1002/2016RS005965, 2016.

Mishin, E., B. Watkins, N. Lehtinen, B. Eliasson, T. Pedersen, and S. Grach, Artificial ionospheric layers driven by high-frequency radiowaves: An assessment, J. Geophys. Res. Space Physics, 121, doi:10.1002/2015JA021823, 2016.

Nigussie, M., S. M. Radicella, B. Damtie, E. Yizengaw, B. Nava, and L. Roininen, Validation of NeQuick TEC data ingestion technique against C/NOFS and EISCAT electron density measurements, Radio Sci., 51, doi:10.1002/2015RS005930, 2016.

Norberg, J., I. I. Virtanen, L. Roininen, J. Vierinen, M. Orispää, K. Kauristie, and M. S. Lehtinen, Bayesian statistical ionospheric tomography improved by incorporating ionosonde measurements, Atmos. Meas. Tech., 9, 1859-1869, doi:10.5194/amt-9-1859-2016, 2016.

Oyama, S.-i., K. Shiokawa, Y. Miyoshi, K. Hosokawa, B. J. Watkins, J. Kurihara, T. T. Tsuda, and C. T. Fallen, Lower-thermospheric wind variations in auroral patches during the substorm recovery phase. J. Geophys. Res. Space Physics, 120, doi: 10.1002/2015JA022129, 2016.

Rietveld, M. T., A. Senior, J. Markkanen, and A. Westman, New capabilities of the upgraded EISCAT high-power HF facility, Radio Sci., 51, 1533-1546, doi:10.1002/2016RS006093, 2016.

Ronksley, A. M., Optical Remote Sensing of Mesoscale Thermospheric Dynamics Above Svalbard and Kiruna, Ph.D. Thesis, University College London, UK, 2016.

Sarno-Smith, L. K., M. Kosch, T. Yeoman, M. Rietveld, A. Nel, and M. Liemohn, Ionospheric Electron Number Densities from CUTLASS dual-frequency Velocity Measurements using artificial backscatter over EISCAT, J. Geophys. Res. Space Physics, 121, doi:10.1002/2016JA022788, 2016.

Sydorenko, D., R. Rankin, and A. W. Yau, Enhanced N2 and O2 densities inferred from EISCAT observations of Pc5 waves and associated electron precipitation, J. Geophys. Res. Space Physics, 120, doi:10.1002/2015JA021508, 2016.

Turunen, E., A. Kero, P. T. Verronen, Y. Miyoshi, S.-I. Oyama, and S. Saito, Mesospheric ozone destruction by high-energy electron precipitation associated with pulsating aurora, J. Geophys. Res. Atmos., 121, 11,852–11,861, doi:10.1002/2016JD025015, 2016.

Tsuda, T., M. Yamamoto, H. Hashiguchi, K. Shiokawa, Y. Ogawa, S. Nozawa, H. Miyaoka, and A. Yoshikawa, A proposal on the study of solar-terrestrial coupling processes with atmospheric radars and ground-based observation network, Radio Sci., , doi:10.1002/2016RS006035, 2016.

Vanhamäki, H., A. Aikio, M. Voiculescu, L. Juusola, T. Nygrén, and R. Kuula, Electrodynamic structure of the morning high-latitude trough region, J. Geophys. Res. Space Physics, 121, doi:10.1002/2015JA022021, 2016.

Voiculescu M., T.J. Nygren, A.T. Aikio, H. Vanhamäki, and V. Pierrard, Post-midnight ionospheric troughs in summer at high latitudes, J. Geophys. Res., 121, doi:10.1002/2016JA023360, 2016.

Wang, X., P. Cannon, C. Zhou, F. Honary, B. Ni, and Z. Zhao, A Theoretical Investigation on the Parametric Instability Excited by X-mode Polarized Electromagnetic Wave at Tromsø, J. Geophys. Res. Space Physics, 121, doi:10.1002/2016JA022411, 2016.

Wang, X., C. Zhou, M. Liu, F. Honary, B. Ni, and Z. Zhao, Parametric instability induced by X-mode wave heating at EISCAT, J. Geophys. Res. Space Physics, 121, doi:10.1002/2016JA023070, 2016.

Wu J, J. Wu, and Z. Xu, Results of ionospheric heating experiments involving an enhancement in electron density in the high latitude ionosphere, Plasma Sci. Technol., 18(5), 890, 2016.

Yamazaki, Y., M.J. Kosch, Y. Ogawa and D.R. Themens, High-latitude ion temperature climatology during the International Polar Year 2007-2008, J. Space Weather Space Clim., 6, A35, 13pp, DOI: http://dx.doi.org/10.1051/swsc/2016029, 2016.

EISCAT Operations 2015 and 2016

The EISCAT radars operate in two basic modes, using approximately half the available observing time for each. In the Special Programme mode, users conduct individual experiments dedicated to specific experiments and objectives. The resulting data are reserved for the exclusive use of the experimenters for one year from the date of collection. Special programmes often make use of the well developed pulse schemes and observing modes of the Common Programme. EISCAT Common Programmes are conducted for the benefit of the entire user community and the resulting data are immediately available to all.

The UHF and VHF radars are often operated simultaneously during the Common Programme experiments. Such observations offer comprehensive data sets for atmospheric, ionospheric, and magnetospheric studies.

Common Programme One, CP-1, uses a fixed transmitting antenna, pointing along the geomagnetic field direction. The three-dimensional velocity and anisotropy in other parameters are measured by means of the VHF receiving stations at Kiruna and Sodankylä. CP-1 is capable of providing results with very good time resolution and is suitable for the study of substorm phenomena, particularly auroral processes where conditions might change rapidly. Continuous electric field measurements are derived from the tri-static F-region data. On longer time scales, CP-1 measurements support studies of diurnal changes, such as atmospheric tides, as well as seasonal and solar-cycle variations.

Common Programme Two, CP-2, is designed to make measurements from a small, rapid transmitter antenna scan. One aim is to identify wave-like phenomena with length and time scales comparable with, or larger than, the scan (a few tens of kilometers and about ten minutes). The first three positions form a triangle with vertical, south, and south-east positions, while the fourth is aligned with the geomagnetic field.

Common Programme Three, CP-3, covers a 10° latitudinal range in the F-region with a 17-position scan up to 74°N in a 30 min cycle. The observations are made in a plane defined by the magnetic meridian through Tromsø. The principal aim of CP-3 is the mapping of ionospheric and electrodynamic parameters over a broad latitude range.

Common Programme Four, CP-4, covers geographic latitudes up to almost 80°N (77°N invariant latitude) using a low elevation, split-beam configuration. CP-4 is particularly suitable for studies of high latitude plasma convection and polar cap phenomena. However, with the present one-beam configuration of the VHF radar, CP-4 is run with either both UHF and VHF radars or with UHF only in a two position scan.

Common Programme Six, CP-6, is designed for low altitude studies, providing spectral measurements at mesospheric heights. Velocity and electron density are derived from the measurements and the spectra contain information on the aeronomy of the mesosphere. Vertical antenna pointing is used.

Common Programme Seven, CP-7, probes high altitudes and is particularly aimed at polar wind studies. The present version, with only one of the VHF klystrons running, is designed to cover altitudes up to 1500 km vertically above Ramfjordmoen.

Equivalent Common Programme modes are available for the EISCAT Svalbard Radar: CP-1 is directed along the geomagnetic field (81.6° inclination). CP-2 uses a four position scan. CP-3 is a 15 position elevation scan with southerly beam swinging positions. CP-4 combines observations in the F-region viewing area with field-aligned and vertical measurements. CP-6 is similar to the mainland radar CP-6. CP-7 is similar to the mainland radar CP-7.

The tables on the next four pages summarise the accounted hours on the various facilities for each month and for each Common Programme mode (CP) or Associate (SP) for the years 2015 and 2016.

KST COMMON PROGRAMMES

2015	Jan	Feb	Mar	Apr	May	Jun	Jul	Aug	Sept	Oct	Nov	Dec	Total	%	Target%
CP1		132	3										135	22	16
CP2			59										59	10	16
CP3			30										30	5	12
CP4			89									171	260	43	10
CP6			27				90						117	19	20
CP7													0	0	18
UP													0	0	
Total	0	132	208	0	0	0	90	0	0	0	0	171	**601**	100	
%	0	22	35	0	0	0	15	0	0	0	0	28	100		

KST SPECIAL PROGRAMMES

2015	Jan	Feb	Mar	Apr	May	Jun	Jul	Aug	Sept	Oct	Nov	Dec	Total	Incl AA	Target
CN				61.5						54.5			116	119	113
FI		7	8.5					8.5			125.5		149.5	152	130
NI		51	17.5								23	31.5	123	126	136
NO	33	34.5	46	12			141		63		21	23	373.5	380	289
SW	23.5	20	33.5					73		21.5	48		219.5	225	226
UK	14.5	16	48.5							3.5	9	4	95.5	99	133
AA					1.5		9		2	4.5	6.5		23.5		
Total	71	128.5	154	73.5	1.5	0	150	81.5	65	84	233	58.5	**1100.5**	**1101**	**1026**
%	6	12	14	7	0	0	14	7	6	8	21	5	100		

	EI	CN	FI	NI	NO	SW	UK	
Target		10.99	12.69	13.26	28.16	21.99	12.92	%

KST OTHER PROGRAMMES

2015	Jan	Feb	Mar	Apr	May	Jun	Jul	Aug	Sept	Oct	Nov	Dec	Total	Target
PP	61		31					30	3.5	18		3	146.5	70
EI			0.5						2			4	6.5	30
RU										26.5	14.5		41	55
FR													0	0
UA		7.5											7.5	0
													0	
													0	
TB													0	0
Total	61	0	31.5	0	0	0	0	30	5.5	44.5	14.5	7	**194**	**155**

KST TOTALS

2015	Jan	Feb	Mar	Apr	May	Jun	Jul	Aug	Sept	Oct	Nov	Dec	Total	Target
CP	0	132	208	0	0	0	90	0	0	0	0	171	601	540
SP	71	128.5	154	73.5	1.5	0	150	81.5	65	84	233	58.5	1100.5	1026
OP	0	0	31.5	0	0	0	0	30	5.5	44.5	14.5	7	133	155
Total	71	260.5	393.5	73.5	1.5	0	240	111.5	70.5	128.5	247.5	236.5	**1834.5**	**1721**

USAGE BREAKDOWN

2015	Jan	Feb	Mar	Apr	May	Jun	Jul	Aug	Sept	Oct	Nov	Dec	Total	Target
UHF	61	188	220.5	35	1.5		69	20	44	89.5	100.5	42	871	547
VHF	58.5	52	114.5	4			101.5	74		3.5	95.5	130.5	634	822
Heating		20	22.5	34			23.5		12	30.5	35	3	180.5	202
Passive KST	49	33.5	146.5				183.5	70			73	243	798.5	600
ESR	0	145.5	120	11.5	3	0	59	0	6	62	142.5	221.5	771	896
Passive ESR													0	

ESR COMMON PROGRAMMES

2015	Jan	Feb	Mar	Apr	May	Jun	Jul	Aug	Sept	Oct	Nov	Dec	Total	%	Target%
CP1		31	60	8.5	3						6		108.5	30	54
CP2		50							6				56	15	16
CP3													0	0	12
CP4			29									111	140	39	10
CP6							59						59	16	
CP7													0	0	
UP													0	0	
Total	0	81	89	8.5	3	0	59	0	6	0	6	111	**363.5**	100	
%	0	22	24	2	1	0	16	0	2	0	2	31	100		

ESR SPECIAL PROGRAMMES

2015	Jan	Feb	Mar	Apr	May	Jun	Jul	Aug	Sept	Oct	Nov	Dec	Total	Incl AA	Target
CN										42			42	43	42
FI											56		56	57	49
NI		7									23.5	14	44.5	46	51
NO		40	8								24.5	37	109.5	113	108
SW			11									18	29	32	84
UK		12	12							3.5	10	27	64.5	66	49
AA										4	7.5		11.5		
Total	0	59	31	0	0	0	0	0	0	49.5	121.5	96	**357**	**357**	**383**
%	0	17	9	0	0	0	0	0	0	14	34	27	100		

ESR OTHER PROGRAMMES

2015	Jan	Feb	Mar	Apr	May	Jun	Jul	Aug	Sept	Oct	Nov	Dec	Total	Target
PP											15	14.5	29.5	130
EI		1								12.5			13.5	20
RU													0	0
FR		4.5											4.5	0
UA													0	0
													0	0
													0	0
TB				3									3	3
Total	0	5.5	0	3	0	0	0	0	0	12.5	15	14.5	**50.5**	**153**

ESR TOTALS

2015	Jan	Feb	Mar	Apr	May	Jun	Jul	Aug	Sept	Oct	Nov	Dec	Total	Target
CP	0	81	89	8.5	3	0	59	0	6	0	6	111	363.5	360
SP	0	59	31	0	0	0	0	0	0	49.5	121.5	96	357	383
OP	0	5.5	0	3	0	0	0	0	0	12.5	15	14.5	50.5	153
Total	0	145.5	120	11.5	3	0	59	0	6	62	142.5	221.5	**771**	**896**

KST COMMON PROGRAMMES

2016	Jan	Feb	Mar	Apr	May	Jun	Jul	Aug	Sept	Oct	Nov	Dec	Total	%	Target%
CP1			1				5.5			39	1.5		47	6	16
CP2		129											129	16	16
CP3			123										123	15	12
CP4	256										87	98	441	55	10
CP6					4	44	4.5		1				53.5	7	20
CP7									1.5				1.5	0	18
UP													0	0	
Total	256	129	124	0	4	44	10	0	2.5	39	88.5	98	**795**	100	
%	32	16	16	0	1	6	1	0	0	5	11	12	100		

KST SPECIAL PROGRAMMES

2016	Jan	Feb	Mar	Apr	May	Jun	Jul	Aug	Sept	Oct	Nov	Dec	Total	Incl AA	Target
CN									52.5	67			119.5	124	85
FI	33		30							18		15.5	96.5	101	99
NI	47.5	12.5	37.5							10		4.5	112	117	103
NO	21	25	36.5	2			85.5		3	1	13		187	198	219
SW	13	24.5	24.5					27	3	32	28.5	39	191.5	200	171
UK			53									41	94	99	100
AA		21.5	17										38.5		
Total	114.5	83.5	198.5	2	0	0	85.5	27	58.5	128	41.5	100	**839**	**839**	**777**
%	14	10	24	0	0	0	10	3	7	15	5	12	100		

	EI	CN	FI	NI	NO	SW	UK	
Target		10.99	12.69	13.26	28.16	21.99	12.92	%

KST OTHER PROGRAMMES

2016	Jan	Feb	Mar	Apr	May	Jun	Jul	Aug	Sept	Oct	Nov	Dec	Total	Target
PP	8	7	7.5					12		16		9	59.5	130
EI												2.5	2.5	33
RU										38			38	0
FR													0	0
UA													0	0
KR													0	0
TB									12	5	1		18	18
Total	8	7	7.5	0	0	0	0	12	12	59	1	11.5	**118**	**259**

KST TOTALS

2016	Jan	Feb	Mar	Apr	May	Jun	Jul	Aug	Sept	Oct	Nov	Dec	Total	Target
CP	256	129	124	0	4	44	10	0	2.5	39	88.5	98	795	708
SP	114.5	83.5	198.5	2	0	0	85.5	27	58.5	128	41.5	100	839	777
OP	0	7	7.5	0	0	0	0	12	12	59	1	11.5	110	259
Total	370.5	219.5	330	2	4	44	95.5	39	73	226	131	209.5	**1744**	**1743**

USAGE BREAKDOWN

2016	Jan	Feb	Mar	Apr	May	Jun	Jul	Aug	Sept	Oct	Nov	Dec	Total	Target
UHF	74.5	207.5	221				22.5		43	190	34.5	51	844	658
VHF	228.5	9	62	4	4	31	39	29	4.5	3	69	125.5	608.5	733
ESR	204.5	218	131.5	0	7	31.5	7.5	0	0.5	118.5	90.5	164	973.5	877
Heating	3.5		31	2			22		24.5	33	4.5	2	122.5	232
Total Radar	507.5	434.5	414.5	4	11	62.5	69	29	48	311.5	194	340.5	2426	2500
Low Power V						6							6	
Passive KST	366	17.5	73			61	60	11.5	4		134.5	155	882.5	600
Passive ESR													0	

ESR COMMON PROGRAMMES

2016	Jan	Feb	Mar	Apr	May	Jun	Jul	Aug	Sept	Oct	Nov	Dec	Total	%	Target %
CP1	30				4		5.5		0.5	39			79	12	54
CP2		129											129	20	16
CP3			123.5										123.5	19	12
CP4	152										63.5	64	279.5	43	10
CP6						31.5	2				3		36.5	6	
CP7													0	0	
UP													0	0	
Total	182	129	123.5	0	4	31.5	7.5	0	0.5	39	66.5	64	**647.5**	100	
%	28	20	19	0	1	5	1	0	0	6	10	10	100		

ESR SPECIAL PROGRAMMES

2016	Jan	Feb	Mar	Apr	May	Jun	Jul	Aug	Sept	Oct	Nov	Dec	Total	Incl AA	Target
CN													0	2	46
FI										54.5			54.5	56	53
NI	8	10										15	33	35	56
NO		34								2	24		60	64	118
SW		21								3			24	27	92
UK										17		31	48	50	54
AA		7	8										15		
Total	8	72	8	0	0	0	0	0	0	76.5	24	46	**234.5**	**235**	**420**
%	3	31	3	0	0	0	0	0	0	33	10	20	100		

ESR OTHER PROGRAMMES

2016	Jan	Feb	Mar	Apr	May	Jun	Jul	Aug	Sept	Oct	Nov	Dec	Total	Target
PP	14.5	8								3			25.5	70
EI		9										2	11	18
RU													0	0
FR													0	0
UA													0	0
KR												52	52	52
TB					3								3	3
Total	14.5	17	0	0	3	0	0	0	0	3	0	54	**91.5**	**142**

ESR TOTALS

2016	Jan	Feb	Mar	Apr	May	Jun	Jul	Aug	Sept	Oct	Nov	Dec	Total	Target
CP	182	129	123.5	0	4	31.5	7.5	0	0.5	39	66.5	64	647.5	315
SP	8	72	8	0	0	0	0	0	0	76.5	24	46	234.5	420
OP	14.5	17	0	0	3	0	0	0	0	3	0	54	91.5	142
Total	204.5	218	131.5	0	7	31.5	7.5	0	0.5	118.5	90.5	164	**973.5**	**877**

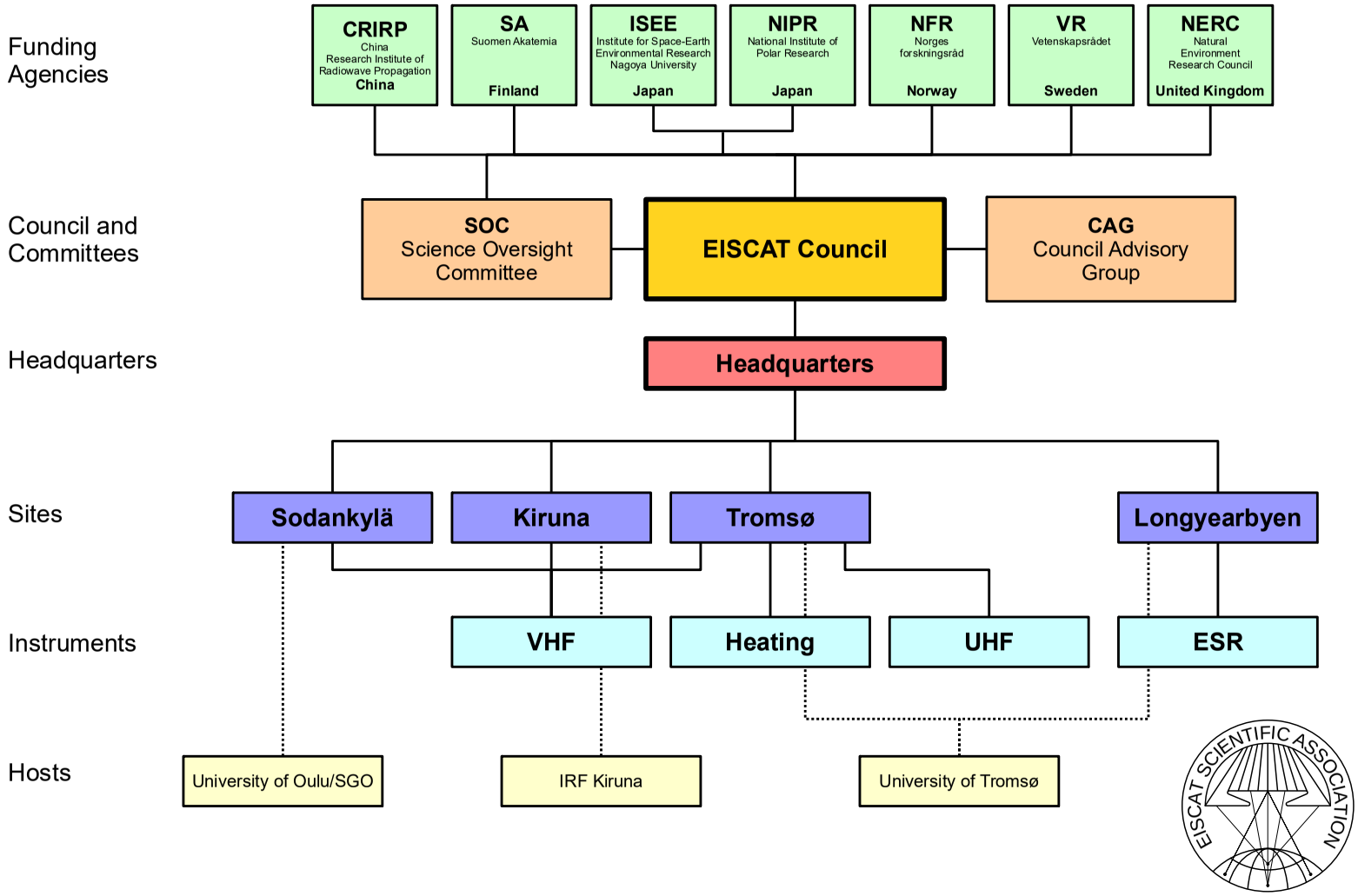

EISCAT organisational diagram, December 2016.

Photo from the Annual Review Meeting, 29 September – 1 October 2015, at Hotel Jussan Topa in Hetta, Finland. From left: Craig Heinselman, Ola Hjelløkken, Carl-Fredrik Enell, Sathyaveer Prasad, Espen Helgesen, Henrik Andersson, Mike Rietveld, Anders Tjulin, Ingemar Häggström, Roger Jacobsen, Lennart Lövqvist, Stian Grande, Ingrid Mann, Arild Stenberg, Elisabet Goth, Erlend Danielsen, Guttorm Mikalsen, Assar Westman.

Photo from the Annual Review Meeting, 18 – 20 October 2016, at Sommarøy Arctic Hotel in Sommarøy, Norway. From left: Hans Erik Fjeld, Erlend Danielsen, Arild Stenberg, Assar Westman, Ola Hjelløkken, Anders Tjulin, Carl-Fredrik Enell, Ingrid Mann, Jussi Markkanen, Roger Jacobsen, Stian Grande, Lennart Lövqvist, Emma Unander, Robert Juhlin, Harri Hellgren, Peter Bergqvist, Mike Rietveld, Elisabet Goth, Henrik Andersson, Craig Heinselman.

EISCAT Scientific Association

December 2016

Council

The Council consists of a Delegation with a maximum of three persons from each Associate.

Finland	
Prof. A. Aikio	
Prof. T. Pulkkinen	
Dr. K. Sulonen	Delegate
Japan	
Dr. H. Miyaoka	*Vice-Chairperson*, Delegate
Dr. S. Nozawa	
Norway	
Prof. A. Brekke	
Dr. B. Jacobsen	Delegate
Dr. L. Lønnum	
P. R. of China	
Dr. Z. Ding	
Prof. Q. Dong	
Prof. J. Wu	Delegate
Sweden	
Dr. T. Andersson	Delegate
Prof. J. Gumbel	
United Kingdom	
Dr. M. Freeman	Delegate
Dr. I. McCrea	*Chairperson*

Scientific Oversight Committee

The EISCAT scientific community organises the Scientific Oversight Committee (SOC), under the guidance of the Council.

Dr. N. Blagoveshchenskaya	Russia (affiliated)
Dr. S. Buchert	*Vice-chairperson*, Sweden
Dr. N. Jakowski	External member
Prof. W. Jun	P. R. of China
Dr. A. Kavanagh	United Kingdom
Prof. C. La Hoz	Norway
Dr. M. Milla	External member
Dr. Y. Ogawa	Japan
Dr. F. Pitout	France (affiliated)
Dr. T. Ulich	*Chairperson*, Finland

Director

Dr. C. Heinselman

Administrative and Finance Committee

The Administrative and Finance Committee (AFC) advises the EISCAT Council on matters relating to administrative, financial and legal issues.

H. Andersson	Head of Administration
M. Friberg	Sweden
C. Heinselman	Director
J. A. Opheim	Norway
A. Kenney	UK
Y. Ohyama	Japan
M. Vannas	*Chairperson*, Finland

Executives

Senior Management

Mr. H. Andersson	Head of Adm., Deputy Dir.
Dr. C. Heinselman	Director

Site Leaders

Station Managers

Mr. R. Jacobsen	Tromsø Radar
Mr. L. Lövqvist	Kiruna Site
Mr. J. Markkanen	Sodankylä Site
Dr. M. Rietveld	Tromsø Heating
Dr. A. Westman	EISCAT Svalbard Radar

Appendix:

EISCAT Scientific Association Annual Report, 2015

EISCAT Scientific Association
Registered as a Swedish non-profit organisation
Organisation number: 897300-2549

Annual report for the financial year 2015-01-01 – 2015-12-31

The EISCAT Council and the Director for the Association submits herewith the annual report for 2015.

ADMINISTRATION REPORT

Ownership, organisation and objective

The EISCAT Scientific Association was established in 1975 through an agreement between six European organisations. Japan joined in 1996 and the Peoples Republic of China in 2007.

The EISCAT Associates at 2015-12-31 are: China Research Institute of Radiowave Propagation (Peoples Republic of China), National Institute of Polar Research (Japan), Natural Environment Research Council (United Kingdom of Great Britain and Northern Ireland), Norges forskningsråd (Norway), Institute for Space-Earth Environment Research, Nagoya University (Japan), Suomen Akatemia (Finland), and Vetenskapsrådet (Sweden).

The now running EISCAT Agreement came into force 2007-01-01, with all Associates making long term funding commitments to the Association. The Association has its formal seat in Kiruna, Sweden, and is registered as a non-profit organisation.

The aim of the Association is to make significant progress in the understanding of physical processes in the high latitude atmosphere by means of experimental programmes generally conducted using the incoherent scatter radar technique, which may be carried out as part of wider international projects. For this purpose, the Association has developed, constructed, and now operates, a number of radar facilities at high latitudes. At present, these comprise a system of stations at Tromsö (Norway), Kiruna (Sweden), Sodankylä (Finland), and Longyearbyen (Svalbard).

The Association is fully funded by the Associates but additional operations may also be funded by short term additional contributions from both Associate and non-Associate bodies. Depending on the available funding, scientific priorities and operational targets are adjusted on an annual basis.

The EISCAT Council is charged with the overall administration and supervision of the Association's activities. The Council appoints a Director, who is responsible for the daily management and operation of the facilities of the Association.

Operation and scientific development

The EISCAT Radars delivered a full programme of operations for the user community and operated reliably throughout the year.

The various EISCAT radars operated for a total of 2 674 accounted hours (2 757 hours in 2014).

Common Programmes amounted to 36% (49%) of the operations. Special Programmes amounted to 55% (43%) and other operations amounted to 9% (8%) of the total hours.

France, Russia, South Korea and Ukraine have affiliate agreements and totally 76 hours (60 hours) were affiliates accounted. The Peer-Review Programme made it possible for users from Belgium, France, Germany, Netherlands, Norway, South Africa, South Korea, Sweden, UK and

USA to run experiments, at no cost, on the systems. Peer-Review time amounted to 176 accounted hours (128 hours).

Future operation and scientific development
All systems are ready for users. These comprise now of the EISCAT Svalbard Radar, Heating and the UHF and VHF radars with the possibility to run the VHF in tristatic mode by using the antennas in Kiruna and Sodankylä for reception.

Project activities
Two EU Framework Programme 7 projects ended in autumn: ESPAS "Near-Earth Space Data Infrastructure for e-Science" and COOPEUS "Strengthening the cooperation between the US and the EC in the field of environmental research infrastructures". The VR-PG "planering av EISCAT_3D" ended at the end of the year.

Three new EU framework programme H2020 projects started: EGI-Engage "Engaging the EGI Community towards an Open Science Commons", EISCAT3D_PfP "EISCAT_3D: Preparation for Production" and ENVRI_Plus "Environmental Research Infrastructures Providing Shared Solutions for Science and Society". A collaborative project between EISCAT and NeIC, Nordforsk (Nordic e-Infrastructure Collaboration) to support EISCAT_3D started as well.

EISCAT3D_PfP has a 3.1 MEUR budget and is a single beneficiary project. Its purpose is to bring the EISCAT_3D concept to industry and have delivery of the first initial units which will be assembled and tested for the first time in an integrated mode. The project started 2015-09-01 and will run for two years. The first year is much about continued planning and initiating industry procurements which will then be delivered and tested in the second year. A test-array comprising of 91 antennas and 182 channels will be assembled at the EISCAT Tromsø site as part of the project.

The MISW "Mitigation of space weather threats to GNSS services" FP7 project and the Vetenskapsrådet (Sweden) funded VR-OG "EISCAT_3D: nästa generations internationella radarsystem för utforskning av atmosfären och den jordnära rymden" continued throughout the year.

The work of the Council and its committees
The Council had two ordinary meetings under the leadership of the new Chairperson, Dr. Ian McCrea. The spring meeting was held in June, in Kiruna, Sweden, and included a site visit to the potential Swedish EISCAT_3D site at Bergfors (located about 40 km NW of Kiruna). The autumn meeting was held on Hainan Island, P. R. of China, early November.

The Scientific Oversight Committee had two meetings during the year. The spring meeting was held in April at the Ångström Laboratory, Uppsala, Sweden and the autumn meeting was held at the South African National Space Agency, in Hemanus, in September. The spring meeting was chaired by Dr. Yasunobu Ogawa and the autumn meeting was chaired by the new Chairperson, Dr. Thomas Ulich.

The adHoc established Administrative and Finance Committee had an introductory meeting in January, in United Kingdom, and two ordinary meetings, at Vetenskapsrådet, Stockholm,

Sweden, in May, and at the Tromsø University, Norway, in October. The first two meetings were chaired by the interim Chairperson, Dr. Ian McCrea. The third meeting was chaired by the new ordinary Chairperson, Mrs. Meri Vannas. During the Tromsø meeting, the Committee visited both the EISCAT Tromsø site and the potential new EISCAT_3D Skibotn location.

The work at both Council and the Committees was much about regular affairs, finalising the updated EISCAT agreement and EISCAT_3D funding activities. The funding negotiations are though largely handled by Associate level round table sittings. One round table meeting was held in 2015. Council renewed also the employment contract with the current Director for another three years starting from 1 January 2016.

Budget development during the year

The 2015 operations ended over the operating target set for the year. The Svalbard radar ran 122 hours less than budgeted and the mainland systems ran 179 hours more than first planned. The user demand remain much on the mainland systems; the UHF and VHF radars and Heating.

The overall spend followed well the prediction for the year and the regular income was well on target. Income from project work, much due to the new EU projects, became better than budgeted. The larger than usual SEK-EUR exchange rate variations towards the end of the year resulted in a financial loss due to value reassessments of received EU prefinancing. The end result became positive.

The long-term budget plan

The long-term budget plan continues to be challenging though now somewhat improved. The five years plan is balanced 2016 - 2019 and the operations will be around 2 500 hours per year during this period. The construction of EISCAT_3D will likely start earliest 2017 and will take five years to complete. The current five years plan do not take this construction, and later operations of the new facilities into account.

The result for 2015 and profit/loss handling

The year was balanced by transferring 2 104 kSEK to the Surplus fund.

PROFIT AND LOSS ACCOUNTS

in thousands of Swedish Crowns

	Note 1	***2015***	***2014***
Associate contributions	Note 2	23 080	21 837
Other operating income		6 631	6 640
		29 711	28 476
Operation costs		-5 529	-5 730
Administration costs		-3 767	-4 139
Personnel costs	Note 3	-18 306	-19 102
Depreciation of fixed assets		-1 802	-1 384
		-29 404	-30 355
Operating profit/loss		*307*	*-1 878*
Interest income		89	61
Other financial income and cost		-325	1 183
Own reserves and funds	Note 4	231	-968
		-5	276
Profit/loss after financial items		*302*	*-1 602*
Appropriations	Note 5	-2 104	218
Transfer from funds invested	Note 6	1 802	1 384
		-302	1 602
Net profit/loss for the year		*0*	*0*

BALANCE SHEET

in thousands of Swedish Crowns

		2015	*2014*
ASSETS			
Fixed assets			
Tangible fixed assets	Note 7		
Buildings		2 265	2 437
Radar systems		5 084	5 765
Equipment and tools		2 847	2 354
		10 196	10 556
Current assets			
Receivables		1 598	5 477
Prepayments and accrued income	Note 8	2 505	8 039
Cash at bank and in hand	Note 9	37 041	22 959
		41 145	36 476
Total assets		*51 341*	*47 032*
CAPITAL AND LIABILITIES			
Capital			
Funds invested	Note 10	10 196	10 556
Funds held on reserve	Note 11	16 241	15 811
		26 437	26 367
Current liabilities			
Liabilities, trade	Note 12	24 586	20 291
Provisions		0	0
Other liabilities		318	373
		24 903	20 664
Total capital and liabilities		*51 341*	*47 032*
Pledged assets		*none*	*none*
Contingent liabilities		*none*	*none*

STATEMENT OF CASH FLOWS

in thousands of Swedish Crowns

	2015	***2014***
Operating activities		
Operating result before financial items	307	-1 878
Transfer from funds invested	1 802	1 384
Interest received	89	61
Currency exchange rate changes	-392	973
Extra ordinary income and cost	67	210
Increase/decrease of receivables	3 879	3 388
Increase/decrease of prepayments and accrued income	5 534	-2 743
Increase/decrease of creditors and liabilities	4 239	-2 266
Cash flow from operations	*15 524*	*-872*
Investment activities		
Investments in tangible assets	-1 443	-6 800
Cash flow from investment activities	*-1 443*	*-6 800*
Cash flow for the year	*14 082*	*-7 672*
Liquid assets at the beginning of the year	*22 959*	*30 631*
Liquid assets at the end of the year	*37 041*	*22 959*

NOTES

Note 1 *Accounting principles*

The accounting and valuation principles applied are consistent with the provisions of the Swedish Annual Accounts Act and generally accepted accounting principles (bokföringsnämnden allmänna råd och vägledningar).

All amounts are in thousands of Swedish kronor (SEK) unless otherwise stated.

Receivables
Receivables are stated at the amounts estimated to be received, based on individual assessment.

Receivables and payables in foreign currencies
Receivables and payables in foreign currencies are valued at the closing day rate. Where hedging measures have been used, such as forwarding contracts, the agreed exchange rate is applied. Gains and losses relating to operations are accounted for under other financial income and cost.

Bank accounts in foreign currencies
Bank balances in foreign currencies are valued at the closing day rate.

Fixed assets
Tangible fixed assets are stated at their original acquisition values after deduction of depreciation according to plan. Assets are depreciated systematically over their estimated useful lives. The following periods of depreciation are applied: Buildings 5 - 50 years, Radar systems 3 - 20 years and Equipment and tools 1 - 5 years.

Note 2 *Associate contributions*

The Associates contributed to the operation during the year in accordance with the agreement. The commitments are in local currencies. The received contributions have been accounted in SEK.

	2015
CRIRP (P. R. of China)	4 013
NIPR (Japan)	1 568
RCN (Norway)	5 617
SA (Finland)	3 553
NERC (United Kingdom)	2 660
VR (Sweden)	5 670
	23 080

Accumulated contributions status as of 2015-12-31
In 2015, both United Kingdom, 166 kSEK, and Sweden, 6 998 kSEK, were credited for providing project related funds.

	1976 - 2015
Previous Associates	382 168
CRIRP (P. R. of China)	29 633
NIPR (Japan)	76 523
RCN (Norway)	167 765
SA (Finland)	78 458
NERC (United Kingdom)	231 614
VR (Sweden)	148 237
	1 114 398

Note 3 *Personnel costs and average number of employees*

The Association employs directly the Headquarters staff, currently about ten positions, including the Director. The Headquarters is located in Kiruna, Sweden. The personnel working at the Kiruna (Sweden), Sodankylä (Finland), Svalbard and Tromsö (Norway) sites are normally not employed by the Association.

	2015	***2014***
Instead, the personnel are provided via site contracts by the Swedish Institute of Space Physics (Kiruna site staff), Oulu University (Sodankylä staff) and Tromsö University (Tromsö and Svalbard staff). The Association refunds all expenses related to the provided staff, as well as an additional overhead.		
Personnel costs in total		
Salaries and emoluments paid to the Director	1 522	1 475
Other personnel, employed and provided via site contracts	11 288	12 084
Social security contributions amounted to	5 060	5 025
of which for pension costs	2 719	2 474

The Director, Dr. Craig Heinselman, started his employment 2013-01-01. Council agreed during the year to renew his employment contract for a further up to three years period.

Of the pension costs, 291 kSEK (283 kSEK) relates to the Director. He and all other directly employed staff are included in ITP like occupational pension plans. For the personnel provided via site contracts, the pension plans are handled by their respective employer.

The members of the board (EISCAT Council) and members of committees, who represents Associates, do not receive remunerations from the Association. Travel expenses in connection with Council and committee meetings are normally covered by the Associates.

Salaries and emoluments and average number of staff per country

Finland		
Salaries and emoluments	634	626
Average number of staff - men and women	1 + 0	1 + 0
Norway (including Svalbard)		
Salaries and emoluments	5 318	5 491
Average number of staff - men and women	9 + 0	9 + 0
Sweden		
Salaries and emoluments	6 858	7 442
Average number of staff - men and women	8 + 2	8 + 2

Members of the board and Directors at year-end - men and women
The board consist of delegations from every Associate country each having a Delegate (formal member) and up to two Representatives.

Board members (EISCAT Council)	11 + 3	11 + 3
Directors	1 + 0	1 + 0

Note 4 *Own reserves and funds*
Transactions involving own reserves and funds.

Capital Operating reserve		
Transfer to the reserve	-765	-1 235
Transfer from the reserve	1 423	4 239
Investments made	-1 443	-6 800
Spare parts reserve		
Transfer to the reserve	-7	-10
Transfer from the reserve	8	37

	2015	2014
Surplus fund		
Transfer from the fund	1 015	2 800
Transfer to the fund	0	0
Sum own reserves and funds	*231*	*-968*

Note 5 *Appropriations*

The outcome for this year became a surplus relative to the budget amounting to 2 104 kSEK. The amount has been transferred to the suplus fund. The 2014 outcome resulted in a deficit (-218 kSEK), which was covered by a transfer from the investment fund.

Note 6 *Transfer from funds invested*

The depreciation cost is covered by funds from Capital - funds invested

Note 7 *Tangible fixed assets*

Changes in tangible fixed assets during 2015.

Buildings		
Opening acquisition value	42 413	42 424
Acquisitions during the year	58	4
Disposals during the year	0	-14
Closing acquisition value	42 471	42 413
Opening accumulated depreciation	-39 976	-39 762
Depreciations during the year	-231	-228
Disposals during the year	0	14
Closing accumulated depreciation	-40 207	-39 976
Closing residual value	2 265	2 437
Radar systems		
Opening acquisition value	250 087	244 693
Acquisitions during the year	0	5 394
Disposals during the year	0	0
Closing acquisition value	250 087	250 087
Opening accumulated depreciation	-244 322	-244 042
Depreciations during the year	-681	-280
Disposals during the year	0	0
Closing accumulated depreciation	-245 002	-244 322
Closing residual value	5 084	5 765
Equipment and tools		
Opening acquisition value	32 649	31 726
Acquisitions during the year	1 384	1 402
Disposals during the year	1 131	480
Closing acquisition value	32 902	32 649
Opening accumulated depreciation	-30 295	-29 899
Depreciations during the year	-891	-876
Disposals during the year	1 131	480
Closing accumulated depreciation	-30 055	-30 295
Closing residual value	2 847	2 354
Sum tangible fixed assets	*10 196*	*10 556*

Note 8 *Prepayments and accrued income*

Resources in staff and direct costs spent in ongoing externally funded projects are covered by accrued income until settled by periodic report claims. In 2015, the ESPAS, COOPEUS and VR-PG projects ended and three new, EGI-Engage, EISCAT3D_PfP and ENVRI_Plus, started.

	2015	2014
Prepaid rents	13	109
Prepaid insurances	633	594
Accrued income, COOPEUS project	0	458
Accrued income, EGI-Engage project	364	0
Accrued income, EISCAT3D_PfP project	491	0
Accrued income, ENVRI_Plus project	222	0
Accrued income, ESPAS project	0	1 312
Accrued income, MISW project	254	173
Accrued income, VR-OG project	329	0
Accrued income, VR-PG project	0	5 312
Other items	199	81
	2 505	8 039

Note 9 *Bank balances status*

Nordea	37 040	22 957
Cash in hand	1	2
	37 041	22 959

Note 10 *Funds invested status*

Buildings	2 265	2 437
Radar Systems	5 084	5 765
Equipment and Tools	2 847	2 354
	10 196	10 556

Note 11 *Funds held on reserve*

Regular investments became higher than budgeted primarily due to partially unexpected car replacements. The surplus for this year (2 104 kSEK) was added to the surplus fund. The other transfers were as budgeted.

Capital operating reserve	1 407	2 065
Equipment repair fund	754	754
Investment fund	7 753	7 753
Restructuring reserve	4 101	4 101
Spare parts reserve	122	122
Surplus fund	2 104	1 015
	16 241	15 811

Note 12 *Liabilities, trade*

All externally funded projects work with prefinancing. For European Commission projects, these are in EUR's. The prefinancing is used to cover reported and approved costs. The ENVRI, EISCAT_3D_2 and VR-PG projects were financially completed during the year. Both the ended COOPEUS and ESPAS projects were still financially open at the end of the year. Prefinancing for the new projects, EGI-Engange, EISCAT3D_PfP and ENVRI_Plus were received.

COOPEUS FP7 prefinancing	1 490	1 522
EGI-Engage H2020 prefinancing	461	0
EISCAT_3D_2 FP7 guarantee fund, whole project	0	2 111
EISCAT_3D_2 FP7 prefinancing	0	1 826
EISCAT3D_PfP H2020 prefinancing	12 909	0
ENVRI FP7 prefinancing	0	484
ENVRI_Plus H2020 prefinancing	1 425	0
ESPAS FP7 prefinancing	468	2 291
MISW FP7 prefinancing	548	519
VR-OG prefinancing	4 000	2 000
VR-PG prefinancing	0	7 000
Liabilities, trade	3 286	2 537
	24 586	20 291

Tromsø 2016-06-01

Dr. Tomas Andersson

Prof. Qing-sheng Dong

Dr. Mervyn Freeman

Dr. Bjørn Jacobsen

Prof. Hiroshi Miyaoka

Dr. Kati Sulonen

Dr. Craig Heinselman
Director

Our audit report was issued on 2016-06-13

Mrs. Annika Wedin
Authorised Public Accountant

Auditor's report

To the council of EISCAT Scientific Association, Corporate Identity Number 897300-2549

Report on the annual accounts

I have audited the annual accounts of EISCAT Scientific Association for the year 2015.

Responsibilities of the council and the director for the annual accounts

The council and the director are responsible for the preparation and fair presentation of the annual accounts in accordance with the Annual Accounts Act, and for such internal control as the council and the director determine is necessary to enable the preparation of annual accounts that are free from material misstatement, whether due to fraud or error.

Auditor's responsibility

My responsibility is to express an opinion on the annual accounts based on my audit. I conducted my audit in accordance with International Standards on Auditing and generally accepted auditing standards in Sweden. Those standards require that I comply with ethical requirements and plan and perform the audit to obtain reasonable assurance about whether the annual accounts are free from material misstatement.

An audit involves performing procedures to obtain audit evidence about the amounts and disclosures in the annual accounts. The procedures selected depend on the auditor's judgment, including the assessment of the risks of material misstatement of the annual accounts, whether due to fraud or error. In making those risk assessments, the auditor considers internal control relevant to the association's preparation and fair presentation of the annual accounts, in order to design audit procedures that are appropriate in the circumstances, but not for the purpose of expressing an opinion on the effectiveness of the association's internal control. An audit also includes evaluating the appropriateness of accounting policies used and the reasonableness of accounting estimates made by the council and the director, as well as evaluating the overall presentation of the annual accounts.

I believe that the audit evidence I have obtained is sufficient and appropriate to provide a basis for my audit opinion.

Opinion

In my opinion, the annual accounts have been prepared in accordance with the Annual Accounts Act and present fairly, in all material respects, the financial position of the association as of 31 December 2015 and its financial performance and its cash flows for the year then ended in accordance with the Annual Accounts Act. The statutory administration report is consistent with the other parts of the annual accounts.

Report on other legal and regulatory requirements

In addition to my audit of the annual accounts, I have also audited the administration of the council and the director of EISCAT Scientific Association for the year 2015.

Responsibilities of the council and the director

The council and the director are responsible for the administration.

Auditor's responsibility

My responsibility is to express an opinion with reasonable assurance on the administration based on my audit. I conducted the audit in accordance with generally accepted auditing standards in Sweden.

As a basis for my opinion on the council and the director´s administration, in addition to my audit of the annual accounts, I examined significant decisions, actions taken and circumstances of the association in order to determine whether any member of the council or the director have undertaken any action or is guilty of negligence which may entail a liability for damages. I also examined whether any council member or the director has, in any other way, acted in contravention of the Annual Accounts Act or the statutes.

I believe that the audit evidence I have obtained is sufficient and appropriate to provide a basis for my opinion.

Opinion

The council and the director have not acted in contravention of the statutes.

Gävle, 13 June 2016

Annika Wedin
Authorized Public Accountant

Appendix:

EISCAT Scientific Association Annual Report, 2016

EISCAT Scientific Association
Registered as a Swedish non-profit organisation
Organisation number: 897300-2549

Annual report for the financial year 2016-01-01 – 2016-12-31

The EISCAT Council and the Director for the Association submits herewith the annual report for 2016.

ADMINISTRATION REPORT

Ownership, organisation and objective
The EISCAT Scientific Association was established in 1975 through an agreement between six European organisations. Japan joined in 1996 and the Peoples Republic of China in 2007.

The EISCAT Associates at 2016-12-31 are: China Research Institute of Radiowave Propagation (Peoples Republic of China), National Institute of Polar Research (Japan), Natural Environment Research Council (United Kingdom of Great Britain and Northern Ireland), Norges forskningsråd (Norway), Institute for Space-Earth Environmental Research, Nagoya University (Japan), Suomen Akatemia (Finland), and Vetenskapsrådet (Sweden).

The now running EISCAT Agreement came into force 2007-01-01, with all Associates making long term funding commitments to the Association. The Association has its formal seat in Kiruna, Sweden, and is registered as a non-profit organisation.

The aim of the Association is to make significant progress in the understanding of physical processes in the high latitude atmosphere by means of experimental programmes generally conducted using the incoherent scatter radar technique, which may be carried out as part of wider international projects. For this purpose, the Association has developed, constructed, and now operates, a number of radar facilities at high latitudes. At present, these comprise a system of stations at Tromsö (Norway), Kiruna (Sweden), Sodankylä (Finland), and Longyearbyen (Svalbard).

The Association is fully funded by the Associates but additional operations may also be funded by short term additional contributions from both Associate and non-Associate bodies. Depending on the available funding, scientific priorities and operational targets are adjusted on an annual basis.

The EISCAT Council is charged with the overall administration and supervision of the Association's activities. The Council appoints a Director, who is responsible for the daily management and operation of the facilities of the Association.

Operation and scientific development
The EISCAT Radars delivered a full programme of operations for the user community and operated reliably throughout the year.

The various EISCAT radars operated for a total of 2 726 accounted hours (2 674 hours in 2015).

Common Programmes amounted to 53% (36%) of the operations. Special Programmes amounted to 39% (55%) and other operations amounted to 8% (9%) of the total hours.

France, Russia, South Korea and Ukraine have affiliate agreements and totally 90 hours (76 hours) were affiliates accounted. The Peer-Review Programme made it possible for users from Japan, Germany, Norway, UK and USA to run experiments, at no cost, on the systems. Peer-Review time amounted to 85 accounted hours (176 hours).

Future operation and scientific development
All systems are ready for users. These comprise now of the EISCAT Svalbard Radar, Heating and the UHF and VHF radars with the possibility to run the VHF in tristatic mode by using the antennas in Kiruna and Sodankylä for reception.

Project activities
The final EU Framework Programme 7 funded project ended in autumn: MISW "Mitigation of space weather threats to GNSS services".

A further EU framework programme H2020 funded project started: COOP_Plus "Cooperation of research infrastructures to address global challenges in the environmental field".

EISCAT is currently participating in four H2020 projects. EISCAT leads, as single beneficiary, the EISCAT3D_PfP project and is partner in the other three projects, COOP_Plus, EGI-Engage and ENVRI_Plus. In addition, EISCAT leads the VR-OG project, funded by Vetenskapsrådet, Sweden and participates in the collaborative NeIC project.

The EISCAT3D_PfP project is now in its second, and final year. Its purpose is to bring the EISCAT_3D concept to industry and have delivery of the first initial units which will be assembled and tested for the first time in an integrated mode. After extensive system modelling work, three main procurement items, First Stager Receiver Unit (FSRU), Antenna Unit (AU) and the Pulse and Steering Control Unit (PSCU), were opened to industry for bids. National Instruments Corporation (with affiliate companies) was selected for the FRSU delivery. Huber+Suhner, represented by its UK branch, was selected as the AU provider. Bids were also received for the PSCU but all were substantially above the expected/budgeted funding target and, hence, the PSCU contract could not be awarded to any of the bidders. A limited-capability prototype version of the PSCU will instead be built in-house by the EISCAT project staff. The FSRU and AU will be delivered to EISCAT Tromsø, where the integrated tests will be performed, during June-July 2017. Additional hardware needed will both be purchased and made in-house, including the PSCU, before the testing starts. The installation of all components will be done May-July followed by a short test period scheduled for August. The EISCAT3D_PfP project ends 31 August 2017.

The work of the Council and its committees
The Council had two ordinary meetings and one follow-up teleconference meeting during the year. The spring meeting was held 1-2 June, at the Arctic University of Norway, Tromsø and included site visits to both the EISCAT Tromsø site and the potential EISCAT_3D site in Skibotn. The autumn meeting was held 2-3 November at Saint Cross College, Oxford, UK. A follow-up Skype meeting was held 14 December. All Council meetings were chaired by Dr. Ian McCrea. The Council work was related both to regular affairs and EISCAT_3D. The follow-up meeting were only about EISCAT_3D funding considerations. The new EISCAT agreement has now been signed by all Associates but one, United Kingdom.

The Scientific Oversight Committee had two meetings during the year. The spring meeting was held 25-26 February, at the University of Oulu, Finland and the autumn meeting was held 14-

15 September, at the Arctic University of Norway. Both meetings were chaired by the Chairperson, Dr. Thomas Ulich.

The adHoc established Administrative and Finance Committee had two meetings during the year. On 27 April, at the Academy of Finland, Helsinki and 12 October, at Weetwood Hall Conference and Hotel, Leeds, UK. The meetings were chaired by Mrs. Meri Vannas.

The EISCAT_3D funding negotiations continued during 2016 and two Associate level round table meetings were held. In January and in November. The EISCAT_3D funding position did not change during the year.

Budget development during the year
The 2016 operations ended slightly over the operating target set for the year. The user demand remain much on the mainland systems. The Svalbard system ran both more common programmes and more system-demanding modes than usual causing a higher electricity use per hour than budgeted.

The overall spend followed otherwise well the prediction for the year and the regular income was close to forecasted. Income from project work became better than budgeted.

In total, the year ended in a deficit which had to be covered by own reserves.

The long-term budget plan
The long-term budget plan continues to be challenging but manageable, in short-term. The five years plan is balanced 2017 - 2020 and the operations will be around 2 500 hours per year during this period. The construction of EISCAT_3D will most probably start in 2017 and will take five years to complete. The current five years plan do not take this construction, and later operations of the new facilities into account.

The result for 2016 and profit/loss handling
The year was balanced by transferring 791 kSEK from the Surplus fund.

PROFIT AND LOSS ACCOUNTS

in thousands of Swedish Crowns

	Note 1	***2016***	***2015***
Associate contributions	Note 2	22 248	23 080
Other operating income		17 250	6 631
		39 498	29 711
Operation costs		-10 276	-5 529
Administration costs		-4 033	-3 767
Personnel costs	Note 3	-21 375	-18 306
Depreciation of fixed assets		-1 983	-1 802
		-37 667	-29 404
Operating profit/loss		*1 831*	*307*
Interest income		6	89
Other financial income and cost		1 004	-325
Own reserves and funds	Note 4	-5 614	231
		-4 605	-5
Profit/loss after financial items		*-2 774*	*302*
Appropriations	Note 5	791	-2 104
Transfer from funds invested	Note 6	1 983	1 802
		2 774	-302
Net profit/loss for the year		*0*	*0*

BALANCE SHEET

in thousands of Swedish Crowns

		2016	2015
ASSETS			
Fixed assets			
Tangible fixed assets	Note 7		
Buildings		2 033	2 265
Radar systems		4 549	5 084
Equipment and tools		2 837	2 847
		9 419	10 196
Current assets			
Receivables		2 385	1 598
Prepayments and accrued income	Note 8	8 530	2 505
Cash at bank and in hand	Note 9	36 318	37 041
		47 233	41 145
Total assets		*56 652*	*51 341*
CAPITAL AND LIABILITIES			
Capital			
Funds invested	Note 10	9 419	10 196
Funds held on reserve	Note 11	19 859	16 241
		29 277	26 437
Current liabilities			
Liabilities, trade	Note 12	26 946	24 586
Other liabilities		429	318
		27 374	24 903
Total capital and liabilities		*56 652*	*51 341*

STATEMENT OF CASH FLOWS

in thousands of Swedish Crowns

	2016	***2015***
Operating activities		
Operating result before financial items	1 831	307
Transfer from funds invested	1 983	1 802
Interest received	6	89
Currency exchange rate changes	1 004	-392
Extra ordinary income and cost	0	67
Increase/decrease of receivables	-786	3 879
Increase/decrease of prepayments and accrued income	-6 025	5 534
Increase/decrease of creditors and liabilities	2 471	4 239
Cash flow from operations	*482*	*15 524*
Investment activities		
Investments in tangible assets	-1 206	-1 443
Cash flow from investment activities	*-1 206*	*-1 443*
Cash flow for the year	*-723*	*14 082*
Liquid assets at the beginning of the year	*37 041*	*22 959*
Liquid assets at the end of the year	*36 318*	*37 041*

NOTES

Note 1 *Accounting principles*

The accounting and valuation principles applied are consistent with the provisions of the Swedish Annual Accounts Act and generally accepted accounting principles (bokföringsnämnden allmänna råd och vägledningar).

All amounts are in thousands of Swedish kronor (SEK) unless otherwise stated.

Receivables

Receivables are stated at the amounts estimated to be received, based on individual assessment.

Receivables and payables in foreign currencies

Receivables and payables in foreign currencies are valued at the closing day rate. Where hedging measures have been used, such as forwarding contracts, the agreed exchange rate is applied. Gains and losses relating to operations are accounted for under other financial income and cost.

Bank accounts in foreign currencies

Bank balances in foreign currencies are valued at the closing day rate.

Fixed assets

Tangible fixed assets are stated at their original acquisition values after deduction of depreciation according to plan. Assets are depreciated systematically over their estimated useful lives. The following periods of depreciation are applied: Buildings 5 - 50 years, Radar systems 3 - 20 years and Equipment and tools 1 - 5 years.

Note 2 *Associate contributions*

The Associates contributed to the operation during the year in accordance with the agreement. The commitments are in local currencies. The received contributions have been accounted in SEK.

	2016
CRIRP (P. R. of China)	3 781
NIPR (Japan)	1 667
RCN (Norway)	5 096
SA (Finland)	3 522
NERC (United Kingdom)	2 512
VR (Sweden)	5 670
	22 248

Accumulated contributions status as of 2016-12-31

In 2016, United Kingdom, were credited 101 kSEK for providing recurrent related funds (Heating transmitter tube repair)

	1976 - 2016
Previous Associates	382 168
CRIRP (P. R. of China)	33 413
NIPR (Japan)	78 189
RCN (Norway)	172 861
SA (Finland)	81 980
NERC (United Kingdom)	234 228
VR (Sweden)	153 907
	1 136 747

Note 3 *Personnel costs and average number of employees*

The Association employs directly the Headquarters staff, currently about eleven positions, including the Director. Of these, five are on shorter-term project employments. The Headquarters is located in Kiruna, Sweden. The personnel working at the Kiruna (Sweden), Sodankylä (Finland), Svalbard and Tromsö (Norway) sites are normally not employed by the Association.

	2016	***2015***

Instead, the personnel are provided via site contracts by the Swedish Institute of Space Physics (Kiruna site staff), Oulu University (Sodankylä staff) and the Arctic University of Norway (Tromsö and Svalbard staff). The Association refunds all expenses related to the provided staff, as well as an additional overhead.

Personnel costs in total

Salaries and emoluments paid to the Director	1 831	1 522
Other personnel, employed and provided via site contracts	13 078	11 288
Social security contributions amounted to	5 920	5 060
of which for pension costs	2 986	2 719

The Director, Dr. Craig Heinselman, started his employment 2013-01-01. His current employment contract ends 2018-12-31.

Of the pension costs, 295 kSEK (291 kSEK) relates to the Director. He and all other directly employed staff are included in ITP like occupational pension plans. For the personnel provided via site contracts, the pension plans are handled by their respective employer.

The members of the board (EISCAT Council) and members of committees, who represents Associates, do not receive remunerations from the Association. Travel expenses in connection with Council and committee meetings are normally covered by the Associates.

Salaries and emoluments and average number of staff per country

Finland		
Salaries and emoluments	655	634
Average number of staff - men and women	1 + 0	1 + 0
Norway (including Svalbard)		
Salaries and emoluments	5 924	5 318
Average number of staff - men and women	10 + 0	9 + 0
Sweden		
Salaries and emoluments	8 331	6 858
Average number of staff - men and women	10 + 2	8 + 2

Members of the board and Directors at year-end - men and women

The board consist of delegations from every Associate country each having a Delegate (formal member) and up to two Representatives.

Board members (EISCAT Council)	12 + 3	11 + 3
Directors	1 + 0	1 + 0

Note 4 *Own reserves and funds*

Transactions involving own reserves and funds.

Capital Operating reserve		
Transfer to the reserve	-1 493	-765
Transfer from the reserve	958	1 423
Investments made	-1 206	-1 443
Spare parts reserve		
Transfer to the reserve	-7	-7
Transfer from the reserve	4	8

	2016	2015
Surplus fund		
Transfer from the fund	0	1 015
Transfer to the fund	-3 870	0
Sum own reserves and funds	*-5 614*	*231*

Note 5 *Appropriations*

The outcome for this year became a deficit relative to the budget amounting to -791 kSEK. The loss was covered by a transfer from the suplus fund. The 2015 outcome resulted in a surplus (2 104 kSEK), which was transferred to the surplus fund.

Note 6 *Transfer from funds invested*

The depreciation cost is covered by funds from Capital - funds invested

Note 7 *Tangible fixed assets*

Changes in tangible fixed assets during 2015.

Buildings		
Opening acquisition value	42 471	42 413
Acquisitions during the year	0	58
Disposals during the year	0	0
Closing acquisition value	42 471	42 471
Opening accumulated depreciation	-40 207	-39 976
Depreciations during the year	-232	-231
Disposals during the year	0	0
Closing accumulated depreciation	-40 439	-40 207
Closing residual value	2 033	2 265
Radar systems		
Opening acquisition value	250 087	250 087
Acquisitions during the year	172	0
Disposals during the year	0	0
Closing acquisition value	250 259	250 087
Opening accumulated depreciation	-245 002	-244 322
Depreciations during the year	-707	-681
Disposals during the year	0	0
Closing accumulated depreciation	-245 709	-245 002
Closing residual value	4 549	5 084
Equipment and tools		
Opening acquisition value	32 902	32 649
Acquisitions during the year	1 034	1 384
Disposals during the year	92	1 131
Closing acquisition value	33 844	32 902
Opening accumulated depreciation	-30 055	-30 295
Depreciations during the year	-1 044	-891
Disposals during the year	92	1 131
Closing accumulated depreciation	-31 008	-30 055
Closing residual value	2 837	2 847
Sum tangible fixed assets	*9 419*	*10 196*

Note 8 *Prepayments and accrued income*

Resources in staff and direct costs spent in ongoing externally funded projects are covered by accrued income until settled by periodic report claims. In 2016, the MISW project ended and one new, COOP_Plus, started.

	2016	2015
Prepaid rents	13	13
Prepaid insurances	607	633
Accrued income, COOP_Plus project	93	0
Accrued income, EGI-Engage project	348	364
Accrued income, EISCAT3D_PfP project	5 198	491
Accrued income, ENVRI_Plus project	561	222
Accrued income, MISW project	0	254
Accrued income, VR-OG project	1 626	329
Other items	84	199
	8 530	2 505

Note 9 *Bank balances status*

Nordea	36 317	37 040
Cash in hand	1	1
	36 318	37 041

Note 10 *Funds invested status*

Buildings	2 033	2 265
Radar Systems	4 549	5 084
Equipment and Tools	2 837	2 847
	9 419	10 196

Note 11 *Funds held on reserve*

Regular investments became lower than budgeted since we did not need to add further disk capacity to the data archive. Instead we make use of a tape archive provided by the Norwegian national infrastructure for computational science. The deficit for this year (-791 kSEK) was covered by the surplus fund. The other transfers were as budgeted.

Capital operating reserve	1 942	1 407
Equipment repair fund	754	754
Investment fund	7 753	7 753
Restructuring reserve	4 101	4 101
Spare parts reserve	125	122
Surplus fund	5 183	2 104
	19 859	16 241

Note 12 *Liabilities, trade*

All externally funded projects work with prefinancing. For European Commission projects, these are in EUR's. The prefinancing is used to cover reported and approved costs. The MISW project was financially reported during the year but the final settlement will only happen in 2017. The COOPEUS and ESPAS projects were settled during the year. Prefinancing for the new project, COOP_Plus, was received.

COOPEUS FP7 prefinancing	0	1 490
COOP_Plus H2020 prefinancing	1 181	0
EGI-Engage H2020 prefinancing	479	461
EISCAT3D_PfP H2020 prefinancing	13 406	12 909
ENVRI_Plus H2020 prefinancing	1 480	1 425
ESPAS FP7 prefinancing	0	468
MISW FP7 prefinancing	570	548
VR-OG prefinancing	4 000	4 000
Liabilities, trade	5 830	3 286
	26 946	24 586

Tokyo 2017-05-31

Dr. Tomas Andersson

Dr. Mervyn Freeman

Prof. Ingrid Mann

Prof. Hiroshi Miyaoka

Dr. Kati Sulonen

Prof. Jian Wu

Dr. Craig Heinselman
Director

Our audit report was issued on 2017-06-15.

Mrs. Annika Wedin
Authorised Public Accountant

Auditor's report

To the council of EISCAT Scientific Association, corporate identity number 897300-2549

Report on the annual accounts

Opinion

I have audited the annual accounts of EISCAT Scientific Association for the year 2016.

In my opinion, the annual accounts have been prepared in accordance with the Annual Accounts Act and present fairly, in all material respects, the financial position of EISCAT Scientific Association as of 31 December 2016 and its financial performance and cash flow for the year then ended in accordance with the Annual Accounts Act. The statutory administration report is consistent with the other parts of the annual accounts.

Basis for Opinion

I conducted my audit in accordance with International Standards on Auditing (ISA) and generally accepted auditing standards in Sweden. My responsibilities under those standards are further described in the *Auditor's Responsibilities* section. I am independent of EISCAT Scientific Association in accordance with professional ethics for accountants in Sweden and have otherwise fulfilled my ethical responsibilities in accordance with these requirements.

I believe that the audit evidence I have obtained is sufficient and appropriate to provide a basis for my opinion.

Responsibilities of the council and the director

The council and the director are responsible for the preparation of the annual accounts and that they give a fair presentation in accordance with the Annual Accounts Act. The council and the director are also responsible for such internal control as they determine is necessary to enable the preparation of annual accounts that are free from material misstatement, whether due to fraud or error.

In preparing the annual accounts, the council and the director are responsible for the assessment of the association's ability to continue as a going concern. They disclose, as applicable, matters related to going concern and using the going concern basis of accounting. The going concern basis of accounting is however not applied if the council and the director intends to liquidate the association, to cease operations, or has no realistic alternative but to do so.

Auditor's responsibility

My objectives are to obtain reasonable assurance about whether the annual accounts as a whole are free from material misstatement, whether due to fraud or error, and to issue an auditor's report that includes my opinions. Reasonable assurance is a high level of assurance, but is not a guarantee that an audit conducted in accordance with ISAs and generally accepted auditing standards in Sweden will always detect a material misstatement when it exists. Misstatements can arise from fraud or error and are considered material if, individually or in the aggregate, they could reasonably be expected to influence the economic decisions of users taken on the basis of these annual accounts.

As part of an audit in accordance with ISAs, I exercise professional judgment and maintain professional scepticism throughout the audit. I also:

- Identify and assess the risks of material misstatement of the annual accounts, whether due to fraud or error, design and perform audit procedures responsive to those risks, and obtain audit evidence that is

sufficient and appropriate to provide a basis for my opinions. The risk of not detecting a material misstatement resulting from fraud is higher than for one resulting from error, as fraud may involve collusion, forgery, intentional omissions, misrepresentations, or the override of internal control.

- Obtain an understanding of the association's internal control relevant to my audit in order to design audit procedures that are appropriate in the circumstances, but not for the purpose of expressing an opinion on the effectiveness of the association's internal control.
- Evaluate the appropriateness of accounting policies used and the reasonableness of accounting estimates and related disclosures made by the council and the director.
- Conclude on the appropriateness of the council's and the director's use of the going concern basis of accounting in preparing the annual accounts. I also draw a conclusion, based on the audit evidence obtained, as to whether any material uncertainty exists related to events or conditions that may cast significant doubt on the association's ability to continue as a going concern. If I conclude that a material uncertainty exists, I am required to draw attention in my auditor's report to the related disclosures in the annual accounts or, if such disclosures are inadequate, to modify my opinion about the annual accounts. My conclusions are based on the audit evidence obtained up to the date of my auditor's report. However, future events or conditions may cause the association to cease to continue as a going concern.
- Evaluate the overall presentation, structure and content of the annual accounts, including the disclosures, and whether the annual accounts represent the underlying transactions and events in a manner that achieves fair presentation.

I must inform the council, among other matters, the planned scope and timing of the audit. I must also inform of significant audit findings during my audit, including any significant deficiencies in internal control that I identified.

Report on other legal and regulatory requirements

Opinion

In addition to my audit of the annual accounts, I have also audited the administration of the council and the director of EISCAT Scientific Association for the year 2016. The council and the director have not acted in contravention of the statutes.

Basis for Opinion

I conducted the audit in accordance with generally accepted auditing standards in Sweden. My responsibilities under those standards are further described in the *Auditor's Responsibilities* section. I am independent of EISCAT Scientific Association in accordance with professional ethics for accountants in Sweden and have otherwise fulfilled my ethical responsibilities in accordance with these requirements.

I believe that the audit evidence I have obtained is sufficient and appropriate to provide a basis for my opinion.

Responsibilities of the council and the director

The council and the director are responsible for the association's organization and the administration of the association's affairs.

Auditor's responsibility

My objective concerning the audit of the administration, and thereby my opinion, is to obtain audit evidence to assess with a reasonable degree of assurance whether any member of the council or the director in any material respect:

- has undertaken any action or been guilty of any omission which can give rise to liability to the association, or
- in any other way has acted in contravention of the Annual Accounts Act or the statutes.

Reasonable assurance is a high level of assurance, but is not a guarantee that an audit conducted in accordance with generally accepted auditing standards in Sweden will always detect actions or omissions that can give rise to liability to the association.

As part of an audit in accordance with generally accepted auditing standards in Sweden, I exercise professional judgment and maintain professional scepticism throughout the audit. The examination of the administration is based primarily on the audit of the accounts. Additional audit procedures performed are based on my professional judgment with starting point in risk and materiality. This means that I focus the examination on such actions, areas and relationships that are material for the operations and where deviations and violations would have particular importance for the association's situation. I examine and test decisions undertaken, support for decisions, actions taken and other circumstances that are relevant to my opinion.

Gävle, 15 June 2017

Annika Wedin
Authorized Accountant

Report 2015–2016 of the EISCAT Scientific Association

EISCAT Headquarters
Box 812, SE-981 28 Kiruna, Sweden

Scientific contributions: EISCAT Associates and staff

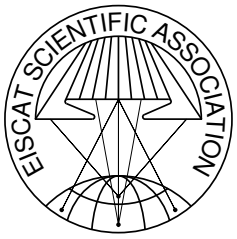

The EISCAT Associates

December 2016

CRIRP
China Research Institute of Radiowave Propagation
China
www.crirp.ac.cn

NERC
Natural Environment Research Council
United Kingdom
www.nerc.ac.uk

NFR
Norges forskningsråd
Norway
www.forskningsradet.no

NIPR
National Institute of Polar Research
Japan
www.nipr.ac.jp

SA
Suomen Akatemia
Finland
www.aka.fi

VR
Vetenskapsrådet
Sweden
www.vr.se

EISCAT Scientific Association

Headquarters

EISCAT Scientific Association
Box 812
SE-981 28 Kiruna, Sweden
Phone: +46 980 79150
www.eiscat.se

Sites

Kiruna

EISCAT Kiruna Site
Box 812
SE-981 28 Kiruna, Sweden
Phone: +46 980 79150

Longyearbyen

EISCAT Svalbard Radar
Postboks 432
N-9171 Longyearbyen, Svalbard
Phone: +47 776 25270

Sodankylä

EISCAT Sodankylä Site
Tähteläntie 54B
FIN-99600 Sodankylä, Finland

Tromsø

EISCAT Tromsø Site
Ramfjordmoen
N-9027 Ramfjordbotn, Norway
Phone: +47 776 20730